ZAKŁAD FIZYKI DOŚWIADCZALNEJ FAZY SKONDENSOWANEJ (ZFDFS)

DEPARTMENT OF EXPERIMENTAL PHYSICS OF CONDENSED PHASE

Skład osobowy / Staff:
prof. dr hab. **Małgorzata Śliwińska-Bartkowiak**
prof. dr hab. **Jan Wąsicki**
prof. dr hab. **Marceli Koralewski**
prof. dr hab. **Marek Szafrański**

dr hab. prof. UAM **Paweł Bilski**
dr hab. prof. UAM **Mateusz Kempiński** (kierownik/head)
dr hab. prof. UAM **Aleksandra Pajzderska**
dr hab. prof. UAM **Maciej Wiesner**

dr **Monika Jażdżewska**
dr **Mikołaj Kościński**

Doktoranci / PhD Students:
mgr **Viktoria Drushliak**, mgr **Sonu Kumar,** mgr **Natalia Przybylska**, mgr **Konrad Rotnicki**, mgr **Anar Rzayev**, mgr **Darko Stojkovski**, mgr **Ephraim Thomas Mathew.**

EXPERIMENTAL PHYSICS

- **Radiospectroscopy: NMR, EPR.**
- **Phase transitions: DSC, dielectric spectroscopy.**
- **Structural methods: X-ray and neutron diffraction.**
- **Spectroscopy, spectrophotometry: visible light, UV, IR.**
- **Surface physics: scanning probe methods (AFM etc.), contact angle measurements, Raman spectroscopy, SNOM.**
- **Charge carrier transport: metals, semiconductors, superconductors, topological insulators, heterostructures.**
- **Phonon transport in 2D systems.**
- **Electron microscopy: SEM, EDS.**
- **Low temperatures, high pressures.**
- **Nanostructure fabrication: physical vapor deposition (PVD), surface structurization, electron lithography.**
- **Numerical simulations: molecular dynamics, density functional theory.**

CONDENSED PHASE – examined systems

- **Crystalline materials: perovskites, ferroelectrics, graphite.**
- **Liquids: "simple" liquids, ionic liquids.**
- **Polymers, microplastics.**
- **2D materials: graphene, transition metal dichalcogenides, intercalated $CrCl_3$ and MoO_3.**
- **Porous structures: active carbons, carbon nanotubes, silica glass.**
- **Pharmacologically active substances: antibiotics, benzodiazepines, dihydropyridines, statines, imidazoles.**

Functional materials for application in various areas, such as: photovoltaics, sensors, filtration, energy storage, chemical nanoreactors, drug delivery, nanoelectronics, spintronics, information storage, nonlinear optics

INTERNATIONAL COOPERATION

- **Paul Scherrer Institute, Villingen Switzerland**
- **Laue Langevin Institute, Grenoble, France**
- **Department of Chemistry and Industrial Chemistry at the University of Piza, Italy**
- **Technical University of Denmark, Lyngby, Denmark**
- **Department of Chemistry, University of Pavia, Italy**
- **Institute of Applied Problems of Physics, NAS of Armenia**
- **MC2 Chalmers University of Technology, Göteborg, Sweden**
- **Microelectronics Research Center, University of Texas at Austin, USA**
- **Texas Materials Institute, Austin, Texas, USA**
- **Institute of Physics, Czech Academy of Sciences, Praha, Czech Republik**
- **Department of Biomolecular and Chemical Emgeneering, North Carolina State University, USA**
- **Department of Bioengineering, Primary Chemical and Biomolecular Engineering. University of Pennsylvania, USA**
- **Institute of Separation Science and Technology, University Erlangen, Germany**
- **Department of Chemistry, Hong-Kong University, China**

POLISH COOPERATION

- **AMU: NanoBioMedical Centre, Faculty of Chemistry, Wielkopolska Center of Advanced Technologies**
- **Institute of Molecular Physics, PAS, Poznan**
- **Poznan University of Technology**
- **Poznan University of Medical Sciences**
- **Poznan University of Life Sciences**
- **Faculty of Physics, University of Białystok**
- **Faculty of Chemistry, UMCS Lublin**
- **Polish Carbon Society**

Structural research of crystalline materials in various thermodynamic conditions

2D perovskite $(CH_3NH_2NH_2)_2PbBr_4$

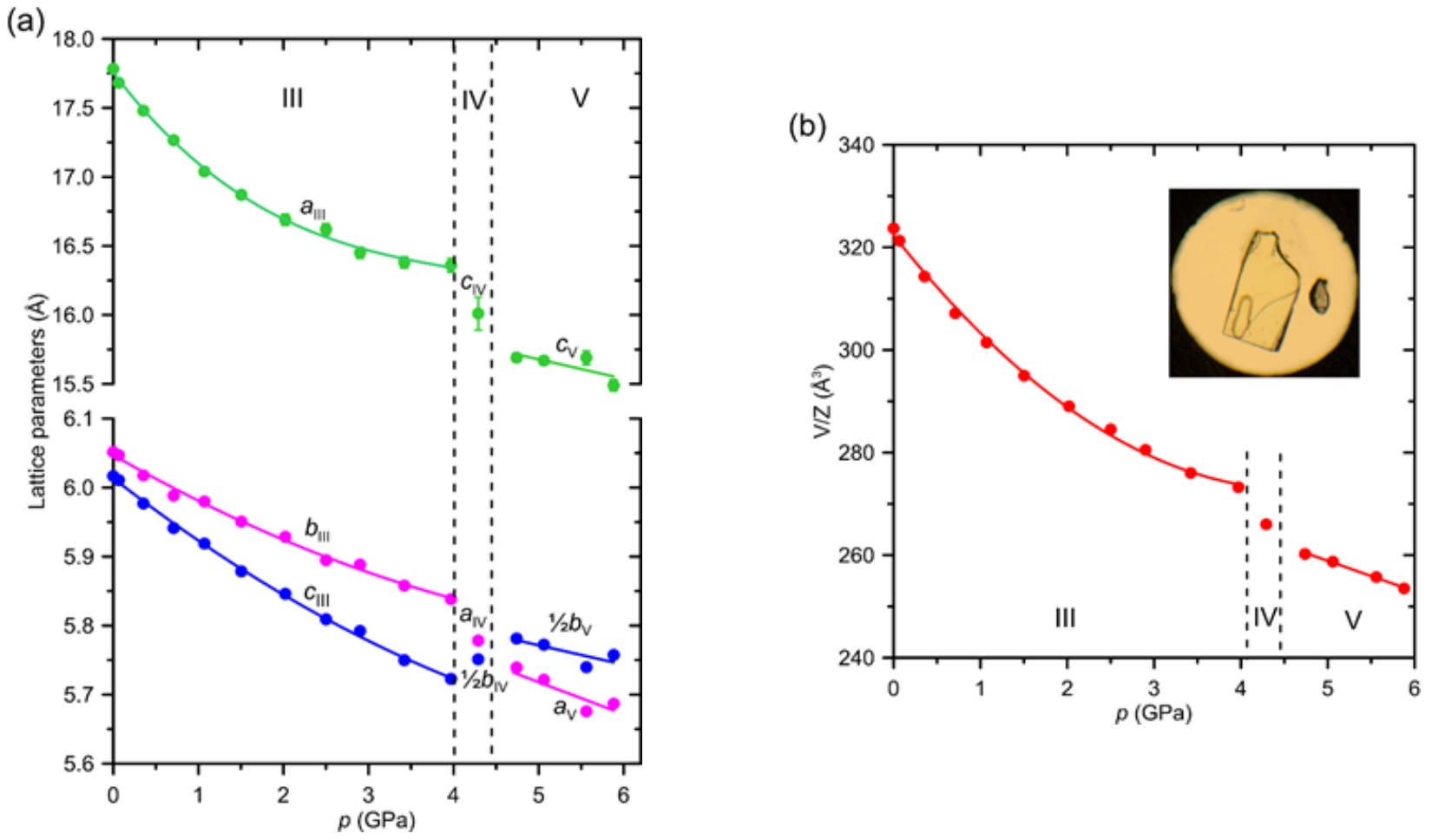

J. Mat. Chem. A 12, 2391 (2024)

2D perovskite $(CH_3NH_2NH_2)_2PbBr_4$

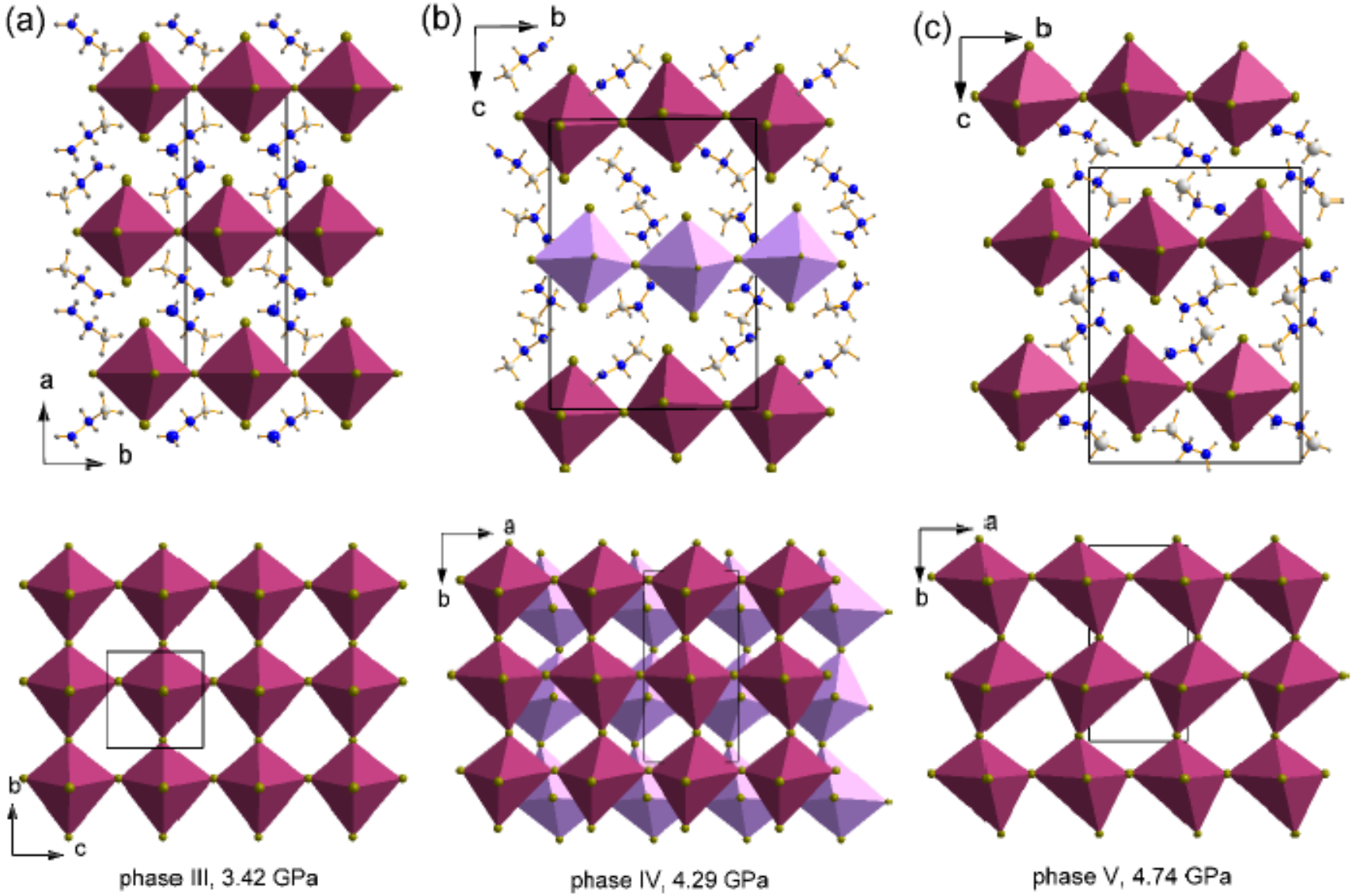

Physical properties of molecular crystals:

optical, ferro- and piezoelectric, multiferroics

Dimethylglycinium-dimethylglycine chloride - new ferroelectric

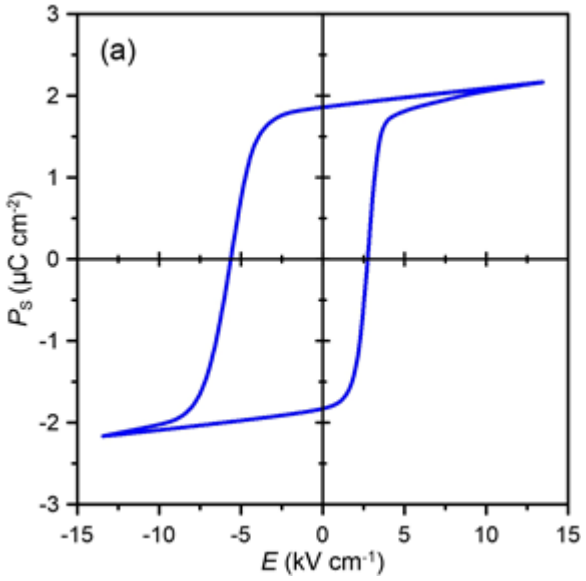

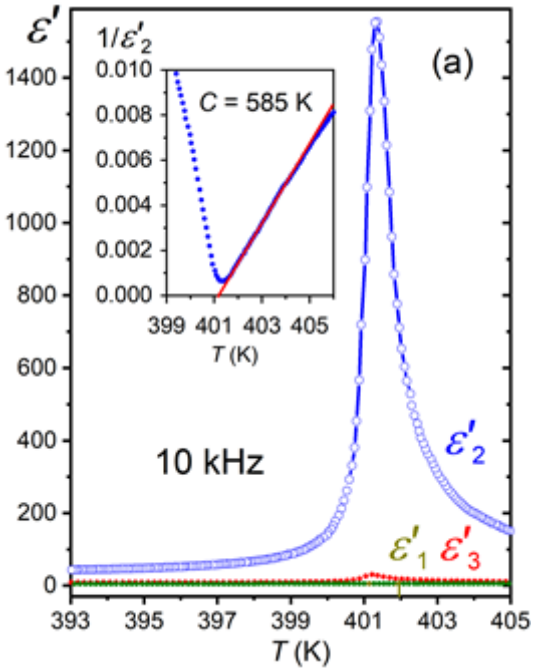

Ferroelectric properties

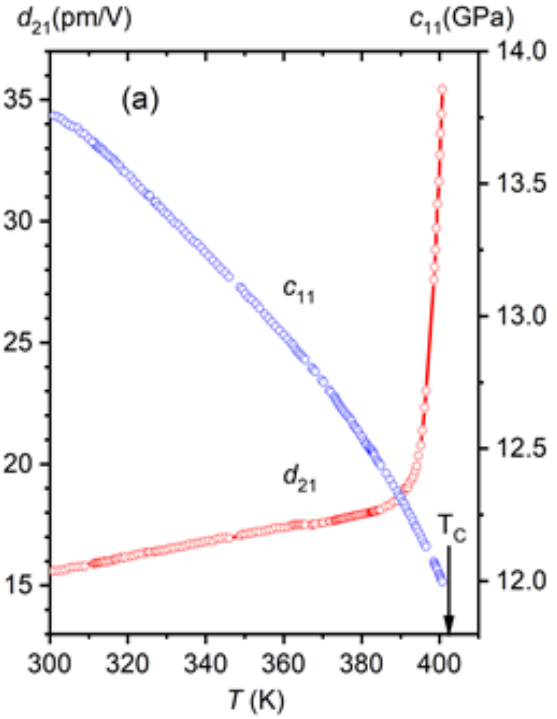

Piezoelectric properties

Mat. Des. 220, 110893 (2022)

X-Ray diffraction on monocrystals as a function of temperature and pressure

Nazwa systemu pomiarowego	**Dyfraktometr rentgenowski Gemini A Ultra, Oxford Diffraction**
Metoda badań	Dyfrakcja rentgenowska na monokryształach
Wyposażenie	• Dwa źródła promieniowania X:Mo-Kα i Cu-Kα • Detektor CCD Atlas • 4-ro kołowy goniometr kappa • Przystawka do pomiarów temperaturowych (zakres temperatur 90 – 500 K) • Komora diamentowe do pomiarów w wysokich ciśnieniach
Możliwości badawcze	• Badania struktury kryształów w warunkach normalnych • Pomiary dylatometryczne i strukturalne w funkcji temperatury • Badania monokryształów w wysokich ciśnieniach hydrostatycznych

Spectrophotometry as a function of pressure and temperature

Nazwa systemu pomiarowego	**Spektrofotometr mikroskopowy MSV-5100, Jasco**
Metoda badań	Badania widma absorpcyjnego w zakresie 200–900 nm
Wyposażenie	• Lampa Xenonowa, Deuterowa, Halogenowa • Przystawka Spectra Academy SV2100 • Obiektyw i kondensor typu Cassegrain x 16
Możliwości badawcze	• Badania widma absorpcyjnego dla ciał stałych o średnicy pola pomiarowego od 10 μm • Opcjonalna możliwość pomiaru fotoluminescencji • Pomiary w świetle spolaryzowanym

3D perovskite $CH_3NH_2NH_2PbBr_3$

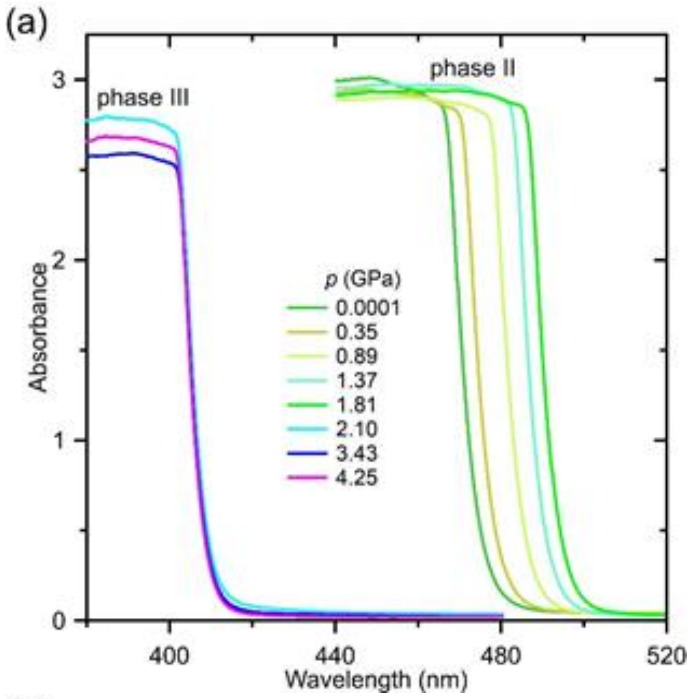

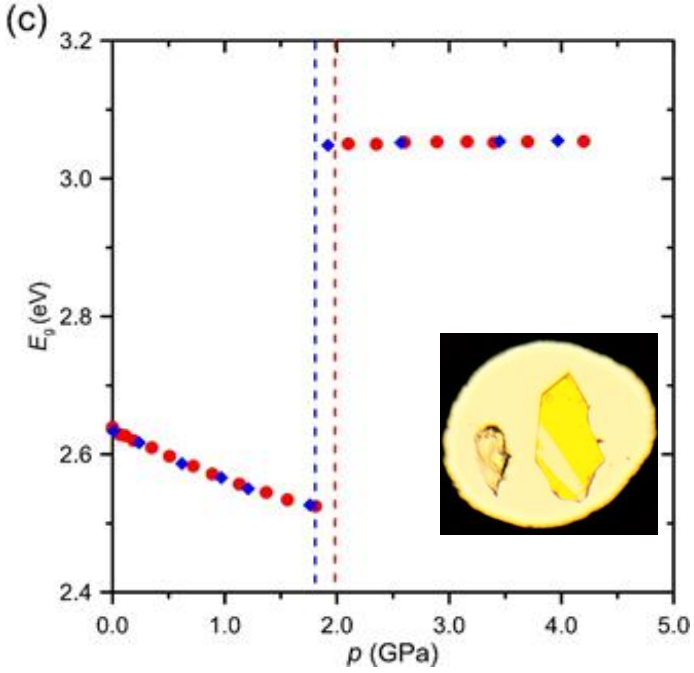

Differential Scanning Calorymetry

Nazwa systemu pomiarowego	**Kalorymetr DSC Q2000, TA Instruments**
Metoda badań	Skaningowa kalorymetria różnicowa
Wyposażenie	• Układ chłodzenia LNCS (zakres od –180 do 550 °C) • Zamknięty układ chłodzenia RSC (zakres od –90 do 550 °C) • Naczynka hermetyczne i typu „low-mass” • Prasa do przygotowania próbek • Automatyczny podajnik próbek
Możliwości badawcze	• Pomiar różnicy strumienia cieplnego między próbką badaną i referencyjną • Pomiar ciepła właściwego • Modulowana analiza DSC

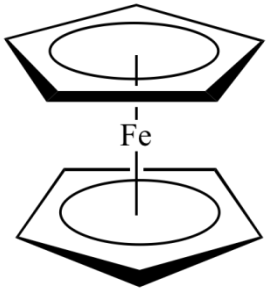

Ferrocene – discovery of modulated phase I"

J. Phys. Chem. Lett. 2023, 14, 3111

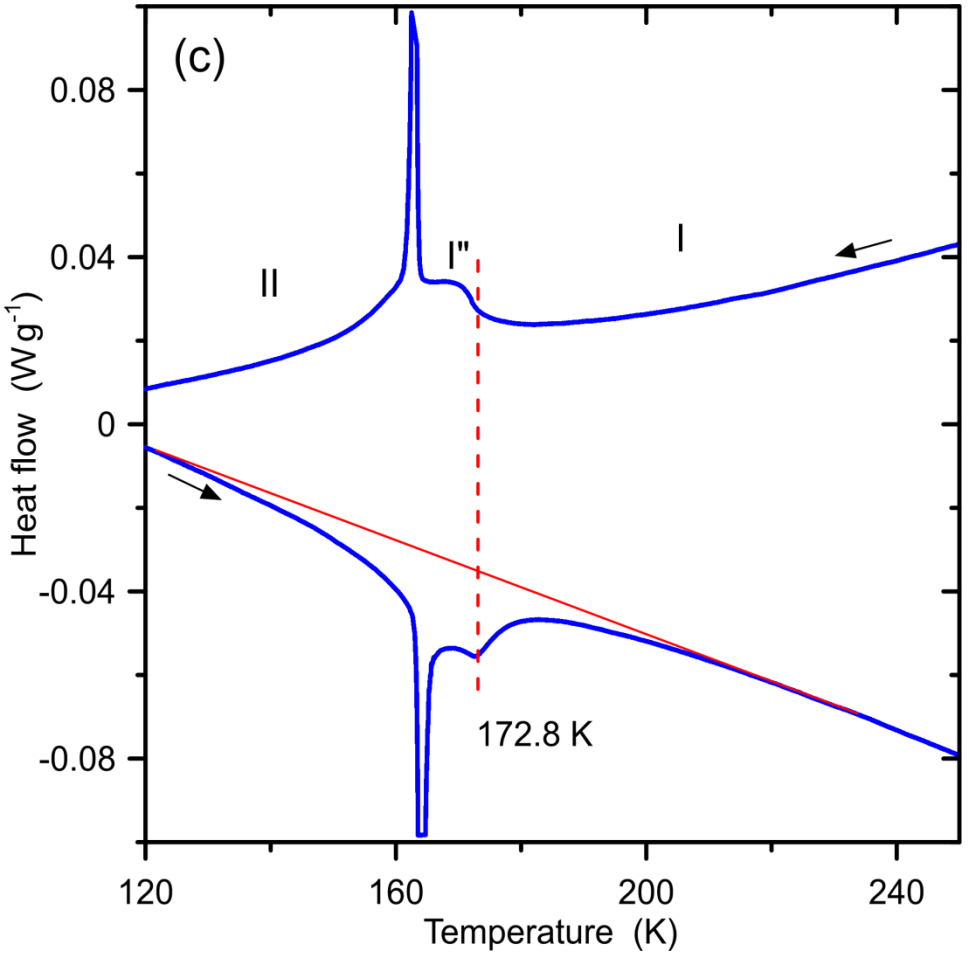

Thermogravimetry

Dabco sulfamate monohydrate (dabco = 1,4-diazabicyclo[2.2.2]octane), $[C_6H_{13}N_2]^+[SO_3NH_2]^-\cdot H_2O$ - dehydratacja oraz rozkład

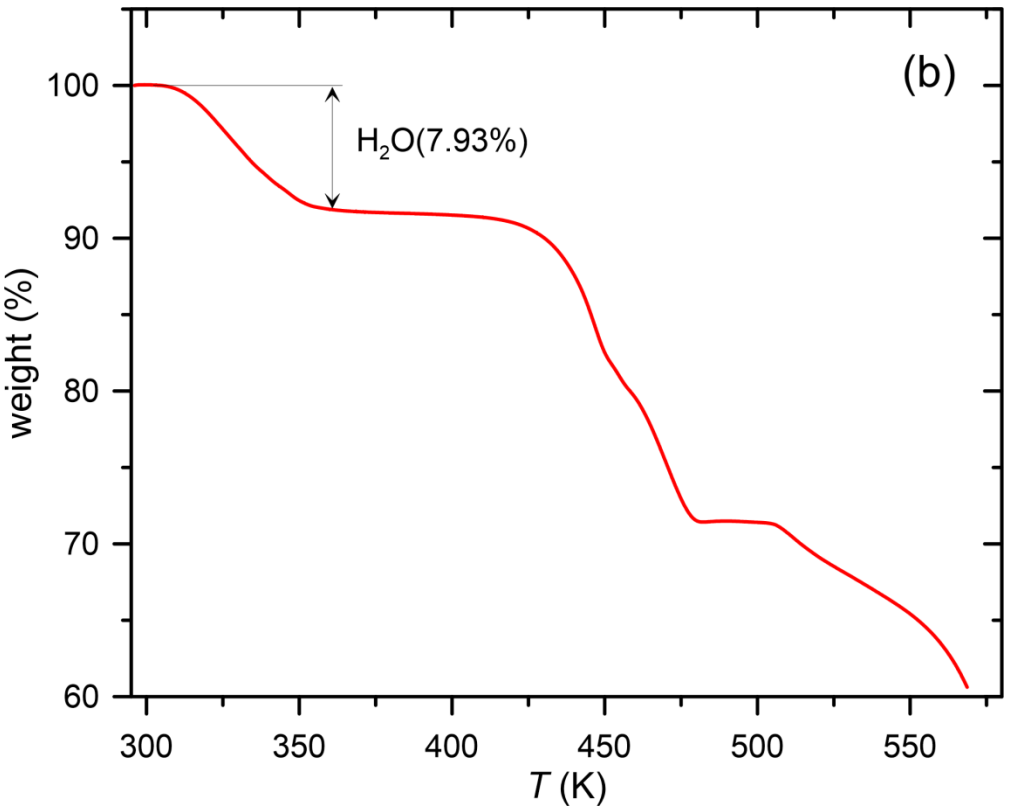

Nazwa systemu pomiarowego	**Analizator termograwimetryczny TGA Q50, TA Instruments**
Metoda badań	Pomiar masy próbki w funkcji temperatury w zakresie od temperatury pokojowej do 1000 ^{O}C
Wyposażenie	• Układ chłodzenia pieca • Masowy kontroler gazu przedmuchującego
Możliwości badawcze	• Badania rozkładu próbki/ubytku masy

Research on molecular reorientations

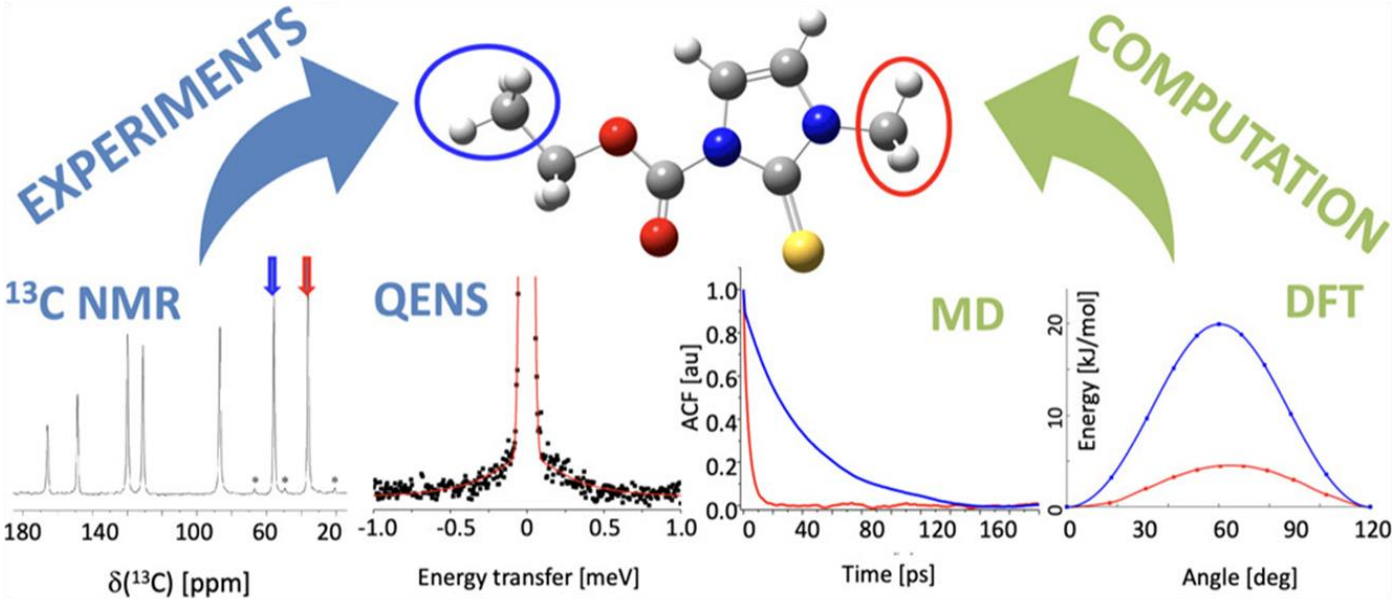

Nuclear magnetic resonance: continuous wave 28 MHz and pulsed 25 MHz – with pressure equipment

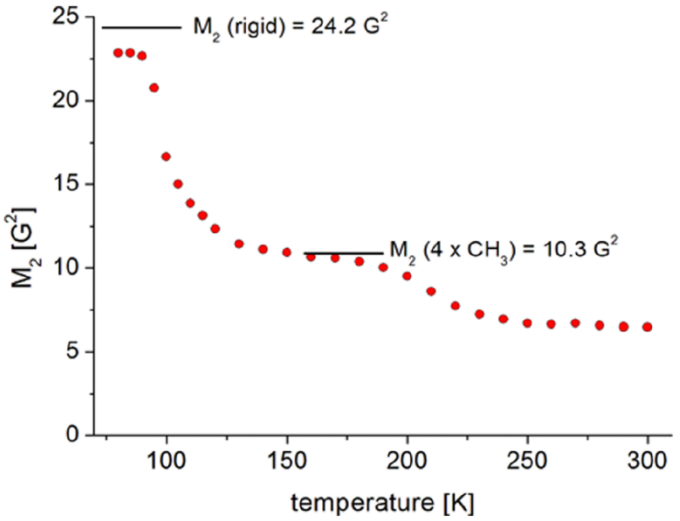

Fig. 6 Second moment of NMR line *versus* temperature for 2,3,3′,4′-tetramethoxy-*trans*-stilbene.

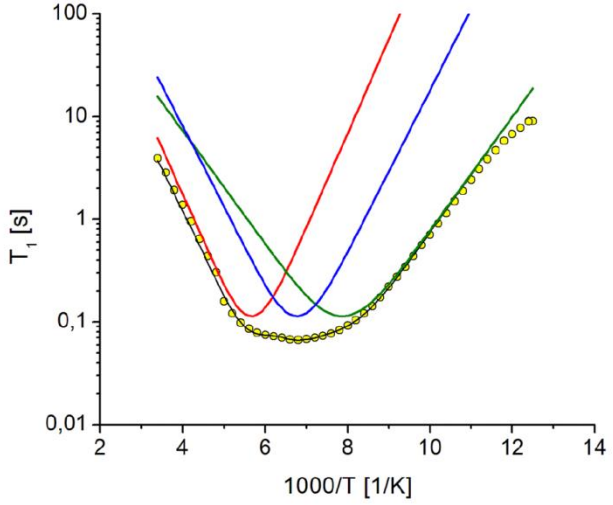

Fig. 7 Spin-lattice relaxation time T_1 for 2,3,3′,4′-tetramethoxy-*trans*-stilbene *versus* inverse temperature and the best fit (solid lines) by equation (1) assuming 3 processes.

Quasi-elastic neutron scattering

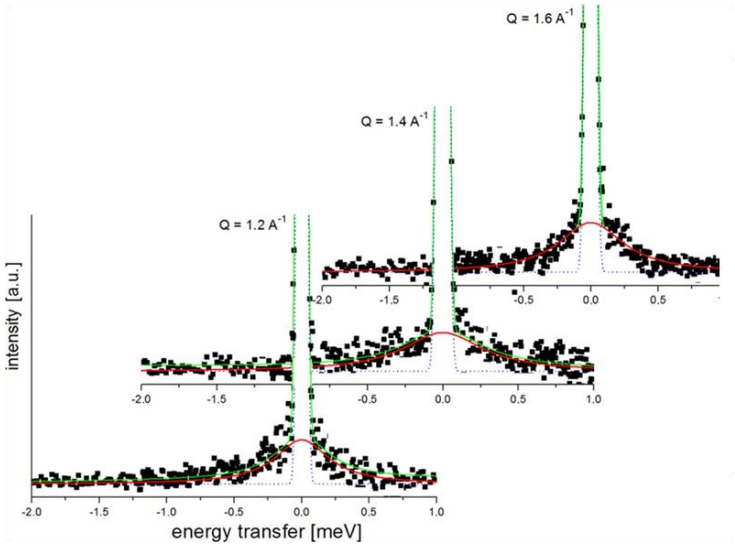

Figure 2. Normalized QENS spectra of carbimazole, recorded on a FOCUS spectrometer at 250 K. The experimental data (black squares) are compared to the fitted model (eq 1, green lines). The individual elastic (blue dotted lines) and the quasielastic (red lines) components are also shown.

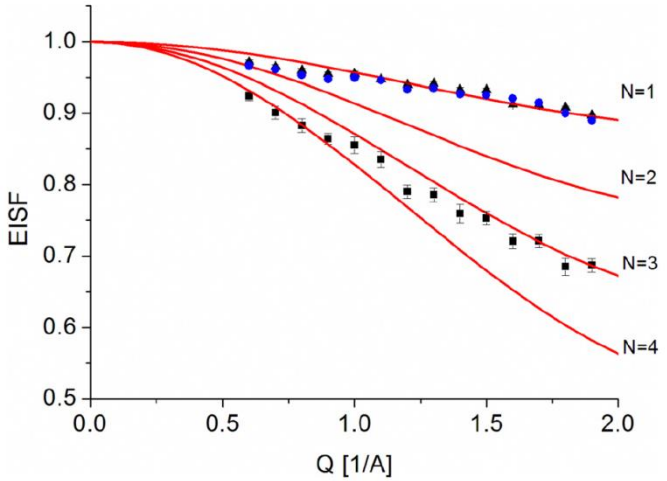

Fig. 10 Experimental EISF of 2,3,3′,4′-tetramethoxy-*trans*-stilbene extracted from QENS data at T = 150 K (triangles), 200 K (circle) and T = 250 K (squares). The solid lines show the theoretical EISF corresponding to the reorientation of N = 1, 2, 3 and 4 methyl groups (eqn (3)).

Molecular dynamics simulations

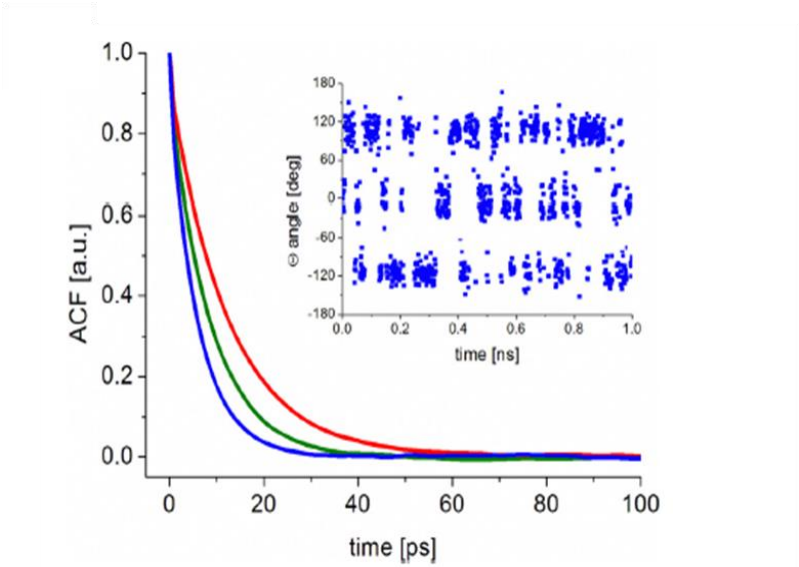

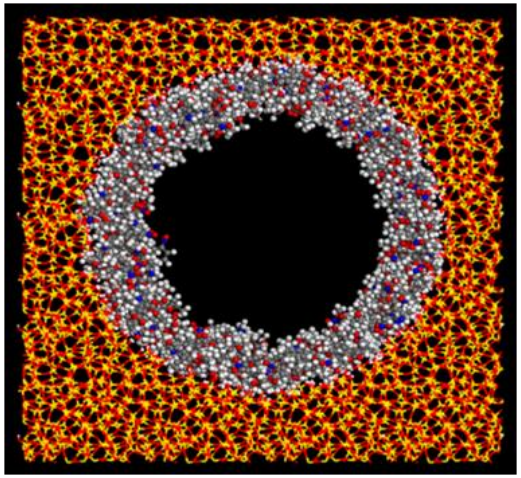

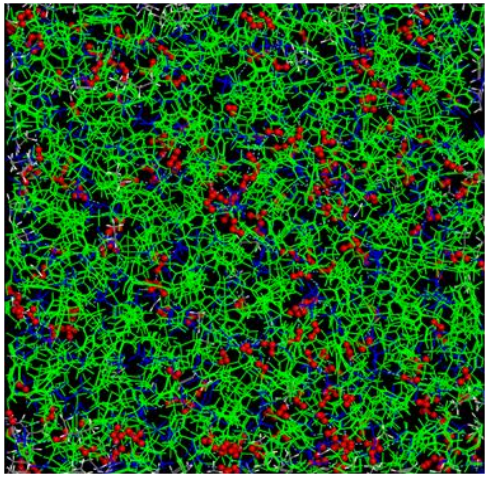

Fig. 13 Angular correlation function corresponding to the reorientation of groups I (red line), II (blue line) and IV (green line) in 2,3,30,40 -tetramethoxy-trans-stilbene. Inset: Time dependence of the torsional angles γ(t) calculated for the randomly chosen methyl group.

Correlation times from NMR, QENS and MD

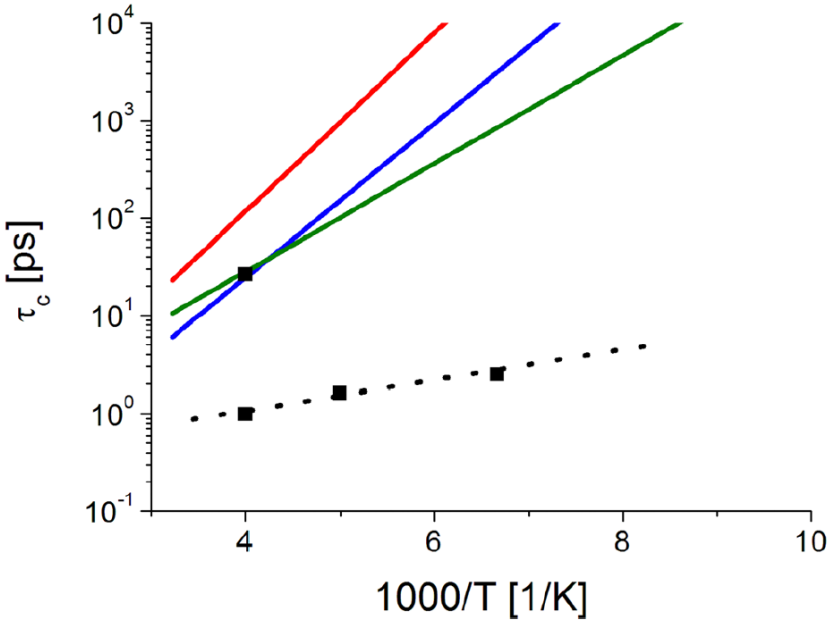

Fig. 11 Correlation times for the reorientational motions of CH_3 groups in 2,3,3′,4′-tetramethoxy-*trans*-stilbene as obtained from QENS (■) and Arrhenius plot from ^{1}H NMR measurements (for E_a = 15.6 kJ mol^{-1} – red line, 12.9 kJ mol^{-1} – blue line, 9.4 kJ mol^{-1} – green line) and QENS data (black, dotted line).

Activation barriers from NMR, QENS, MD and DFT calculations

Table 2 The activation energies of reorientation of CH_3 obtained by ^{1}H and ^{13}C solid-state NMR, QENS, DFT, and MD

No. methyl group	E_a (kJ mol^{-1}) ^{1}H NMR	E_a (kJ mol^{-1}) ^{13}C NMR	E_a (kJ mol^{-1}) QENS	E_a (kJ mol^{-1}) DFT	E_a (kJ mol^{-1}) MD
I	17.5	15.6	—	13.0	13.5
II	15.1	12.9	—	13.1	12.4
III	—		3.0	5.4	3.3
IV	10.6	9.4	—	12.7	9.1

Research on the influence of microplastics on the environment

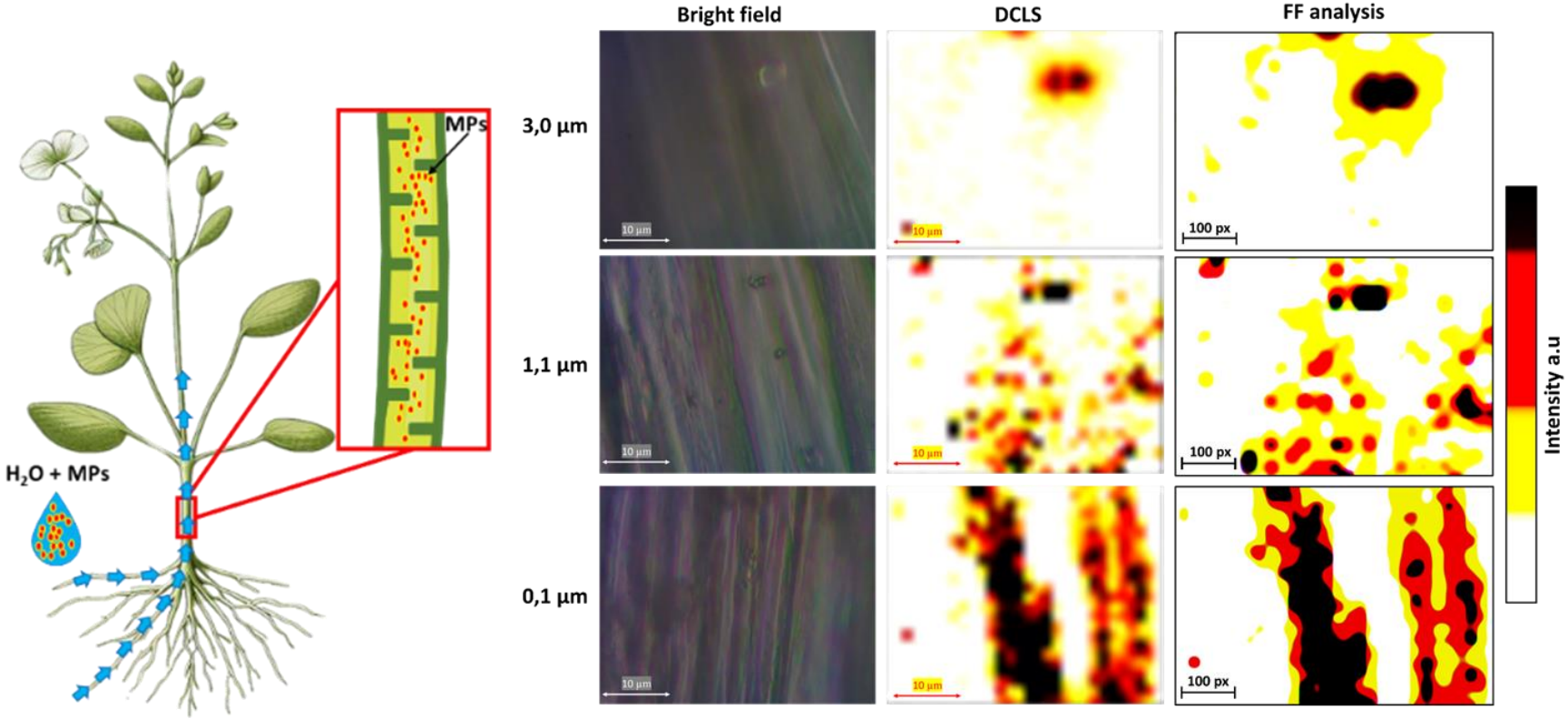

Figure 1 The bright-field microscope image, the Direct Classical Least Squares (DCLS) Raman map and fill factor image of 3.0 µm, 1.1 µm and 0.1 µm polystyren microplastics in cress stem tissue.

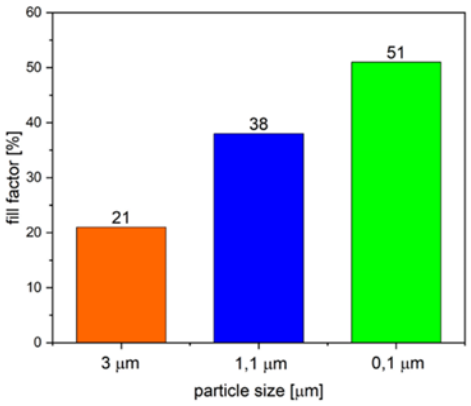

Figure 2. Dependence of the degree fill factor of the cress stalks on the size of the polysterene particles

Research on the influence of microplastics on the environment

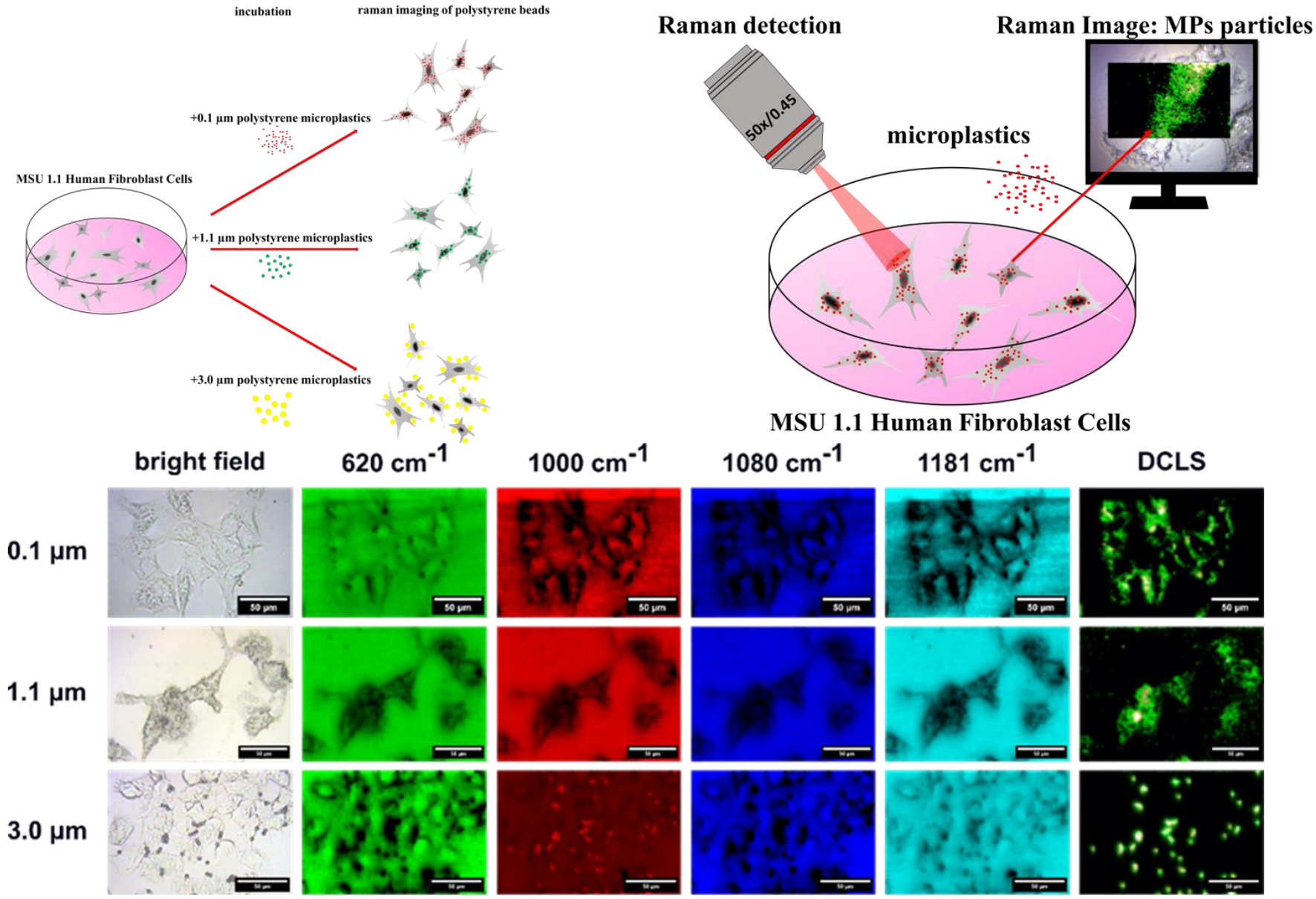

Figure 1. The bright-field microscope image, polystyrene characteristic peaks position images and the Direct Classical Least Squares (DCLS) Raman map of 3.0 μm, 1.1 μm and 0.1 μm in MSU 1.1 Cells

Raman spectroscopy of 2D systems

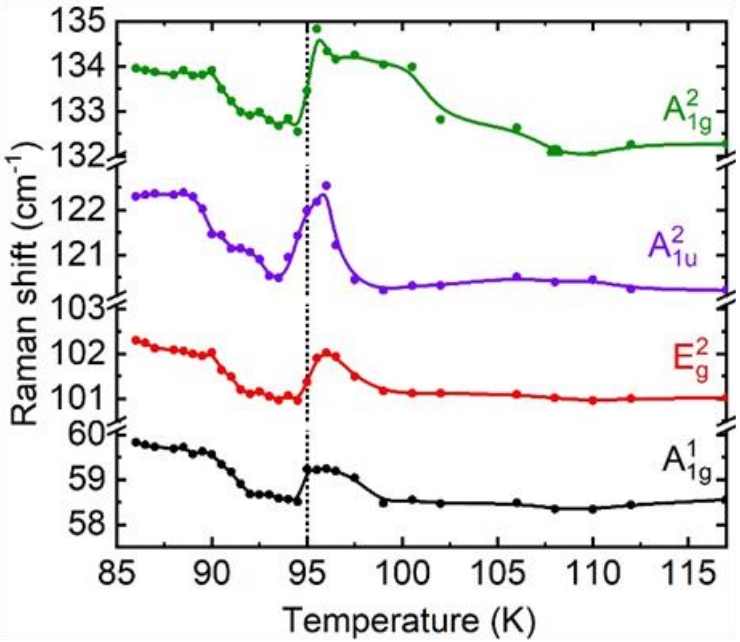

Proximity induced superconductivity in Bi_2Te_3 topological insulator deposited on YBCO semiconductor as evidenced by the change in Raman shift (T_c = 95 K).

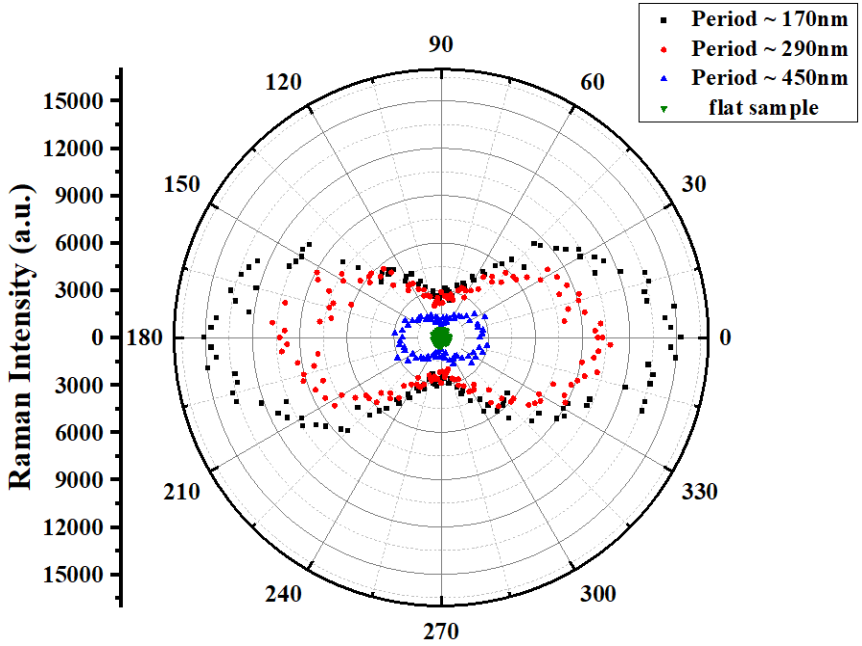

Surface enhanced Raman scattering anisotropy of thiophenol peak due to periodic corrugation of a sapphire substrate

Charge carrier behavior in 2D systems

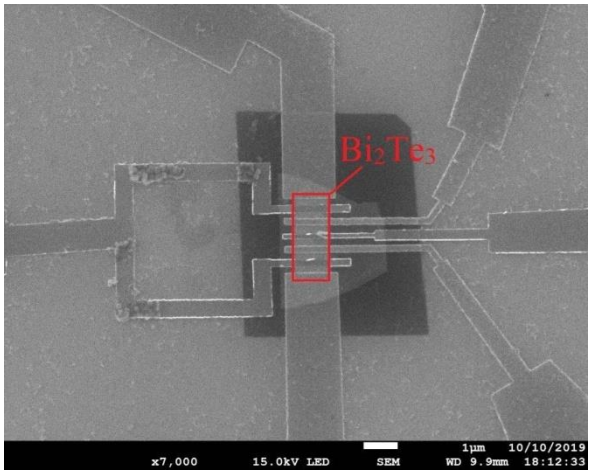

SQUID with topological insulator Bi_2Te_3 as the active element

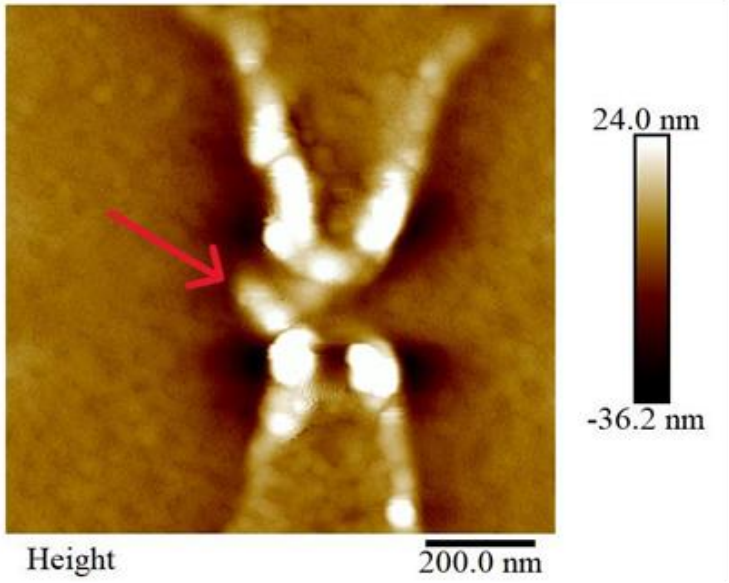

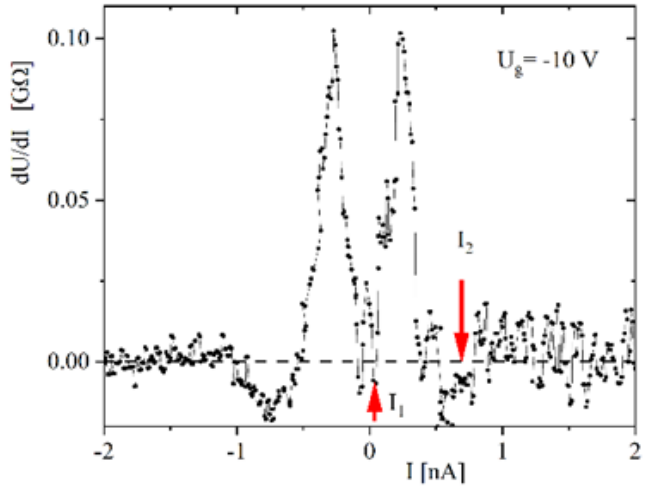

Tunneling of positive and negative carriers (I1 and I2) through DNA molecule anchored between two electrodes.

Charge carrier behavior in disordered graphene-based systems

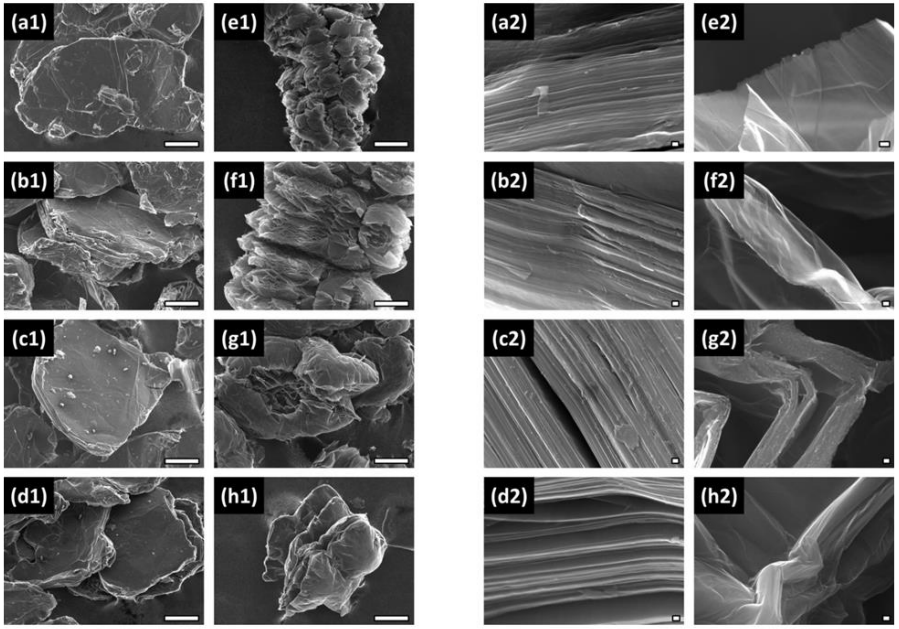

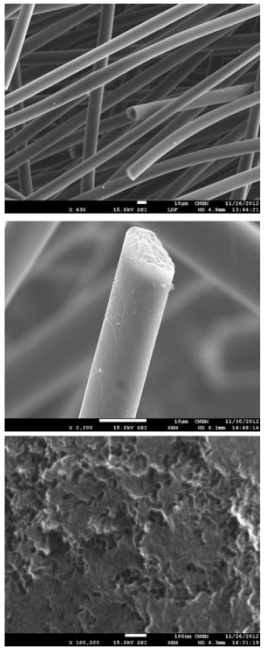

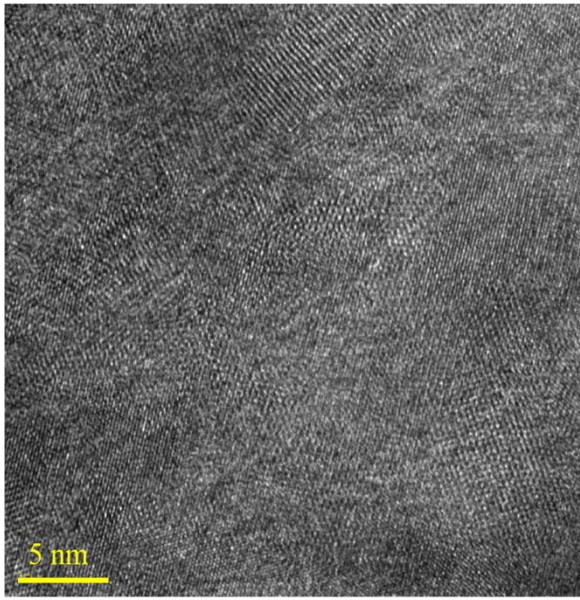

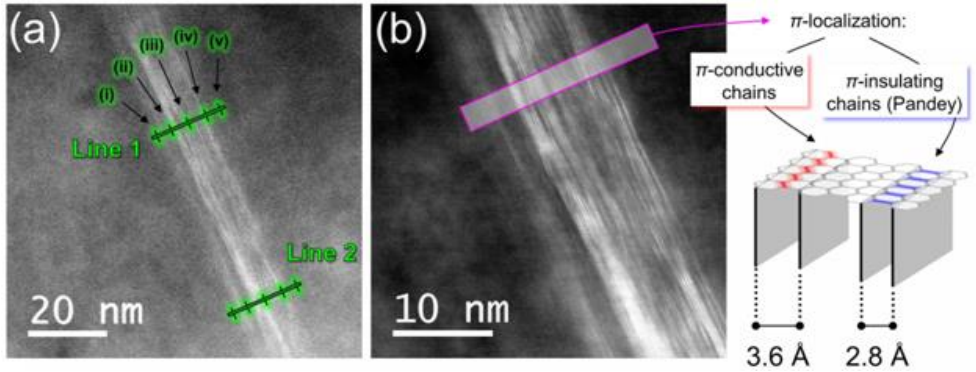

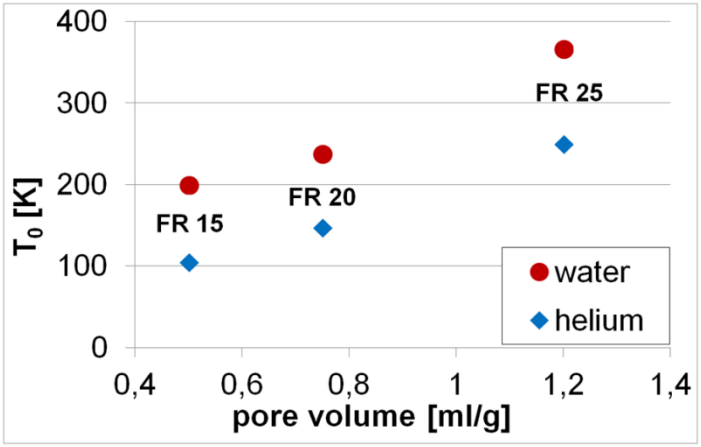

EPR of carbon-based systems

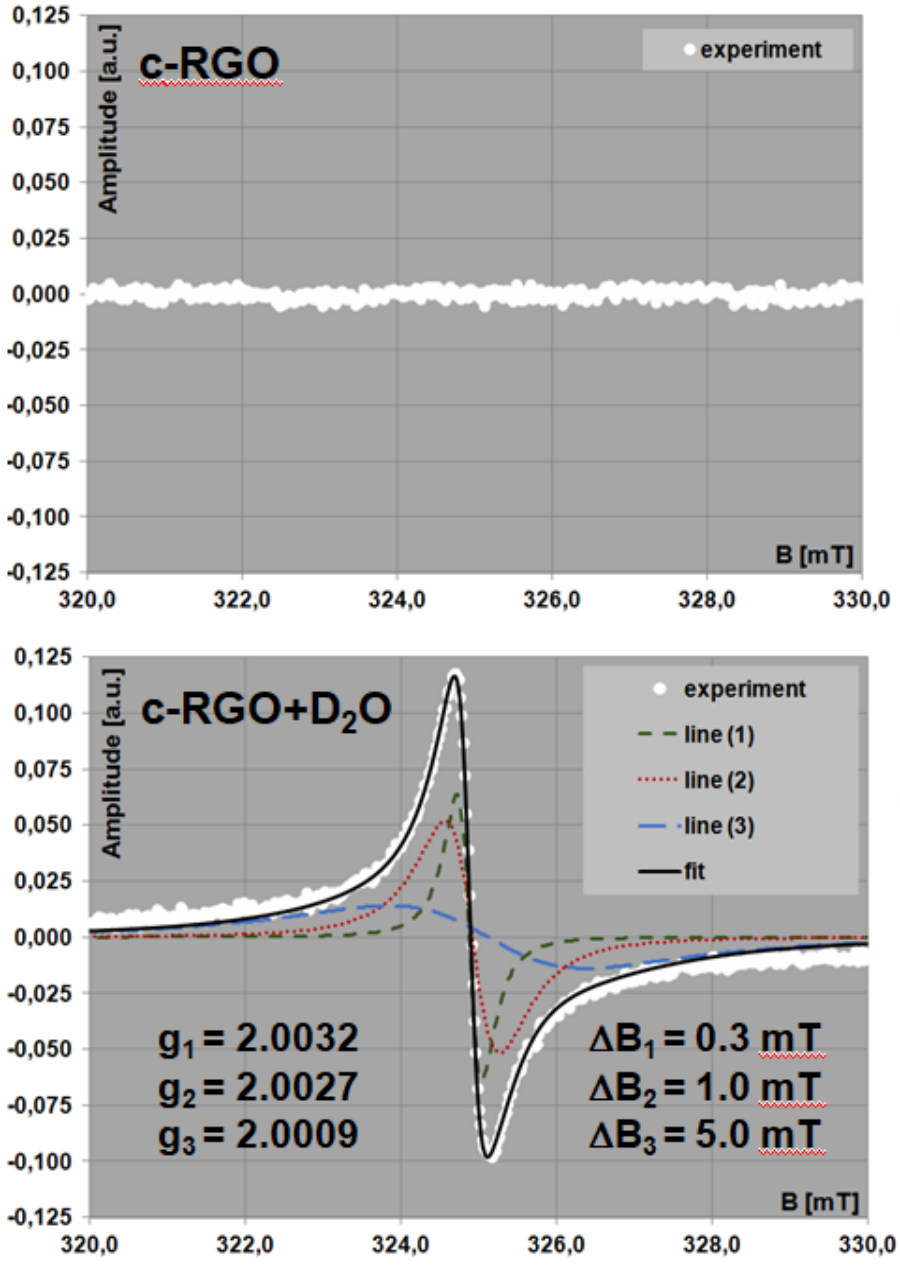

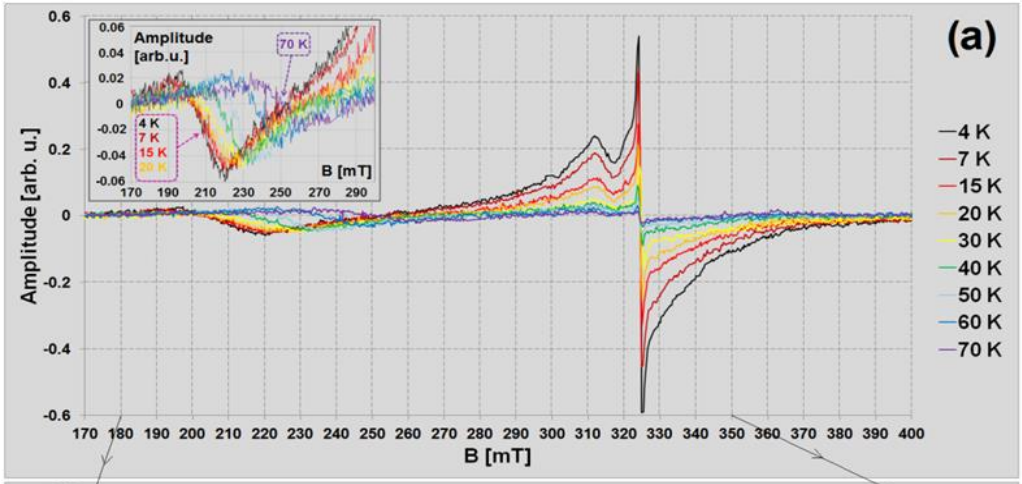

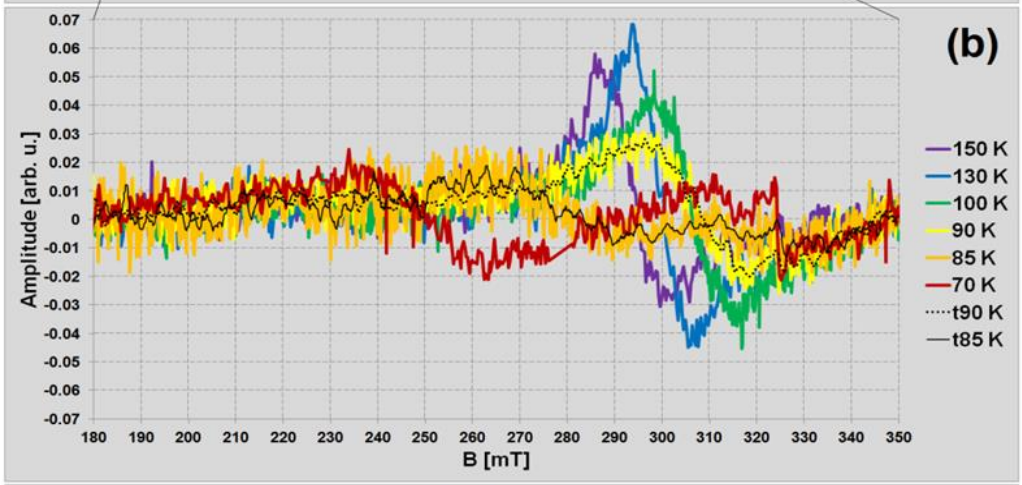

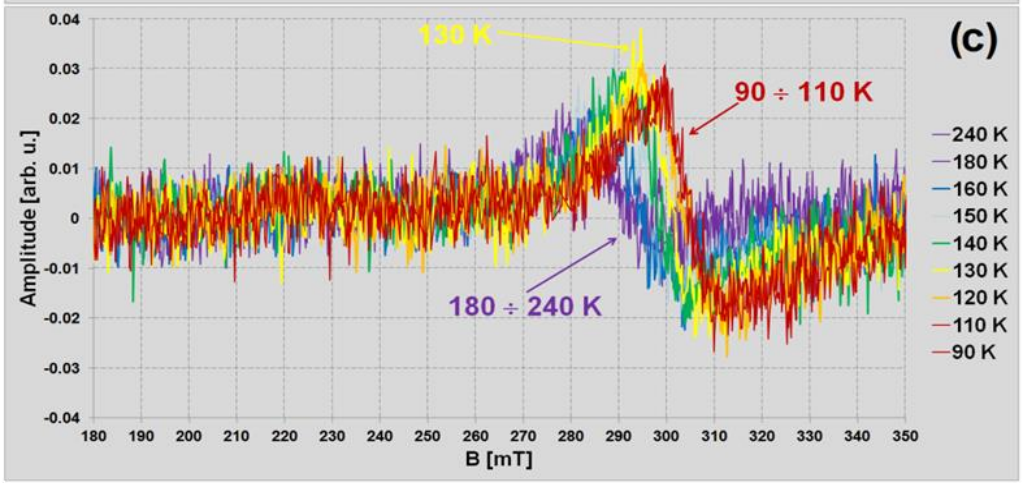

PROTEOX MX

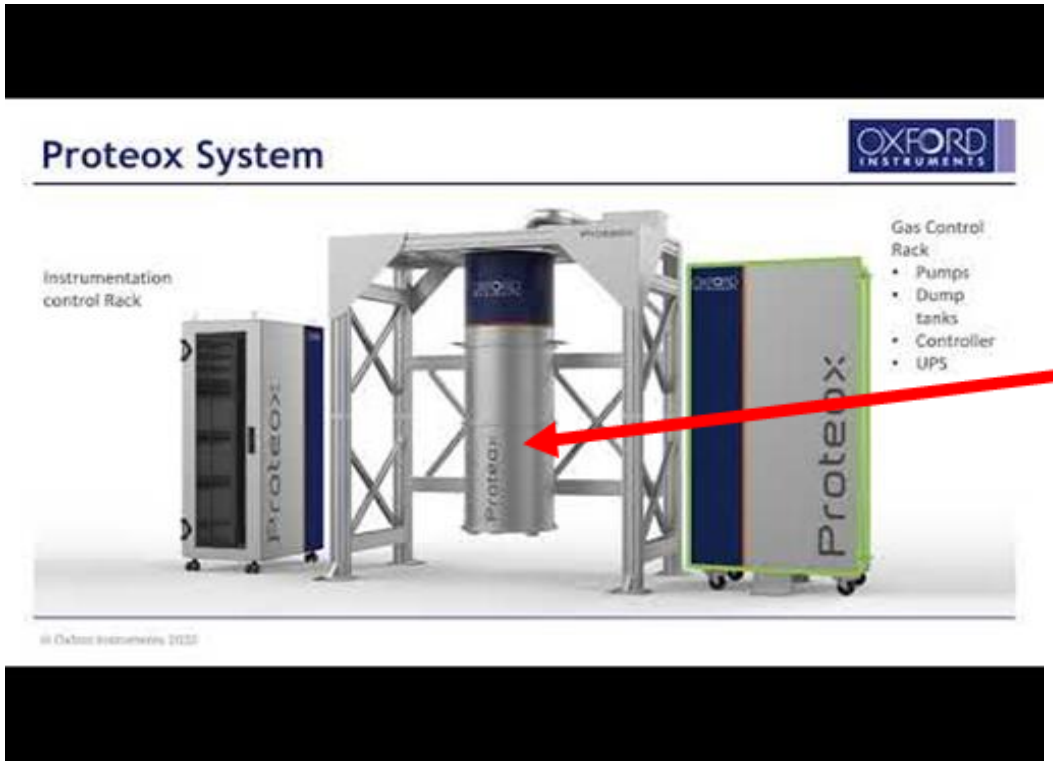

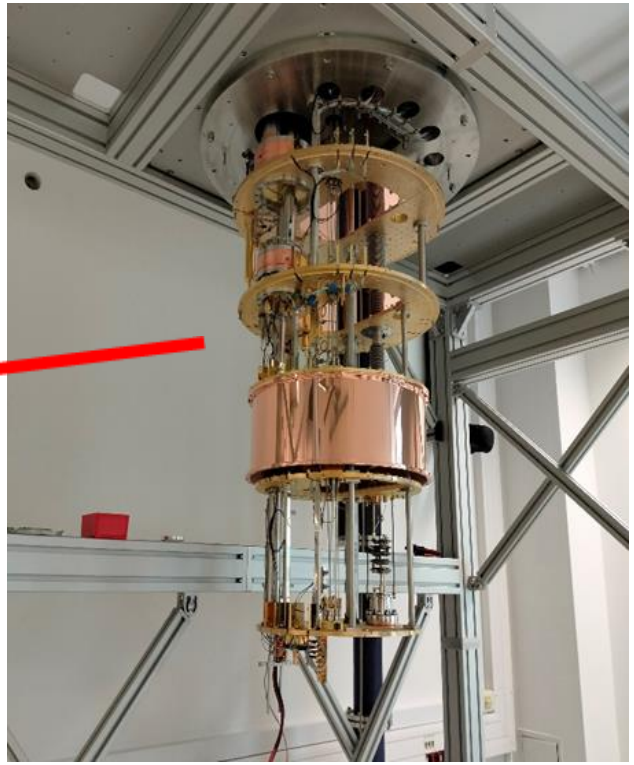

Base temperature 7 mK, magnetic field up to 12 T. Possibility of sweeping the magnetic field in temperature range from 7 mK to 30 K. RF measurements up to 18 GHz,

DC measurements of ultra-low current (fA) and voltage (nV),

impedance measurements up to 5 MHz, impedance module from 1 mΩ to 1 TΩ.

Preparation and analysis of thin films and surface nanostructures

Pulsed laser (ns, fs) modification of metallic surfaces

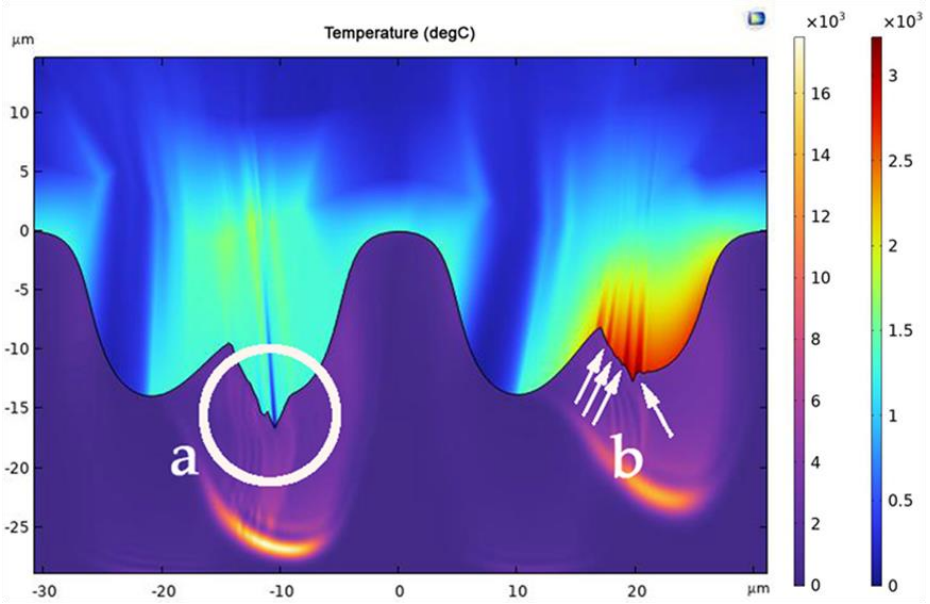

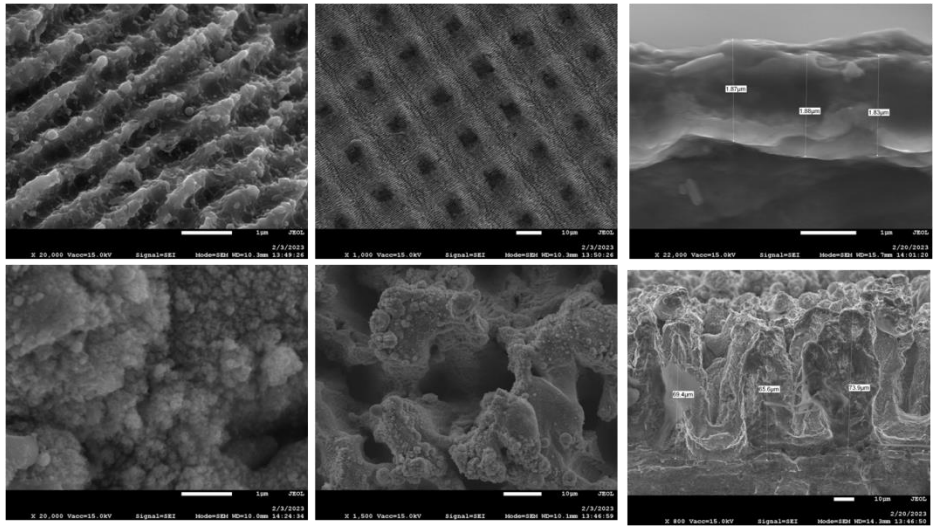

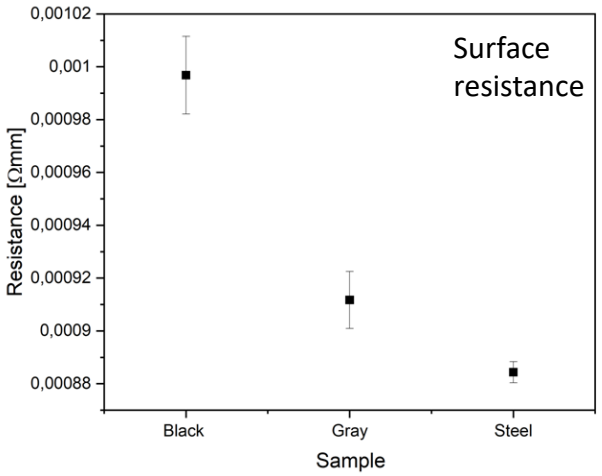

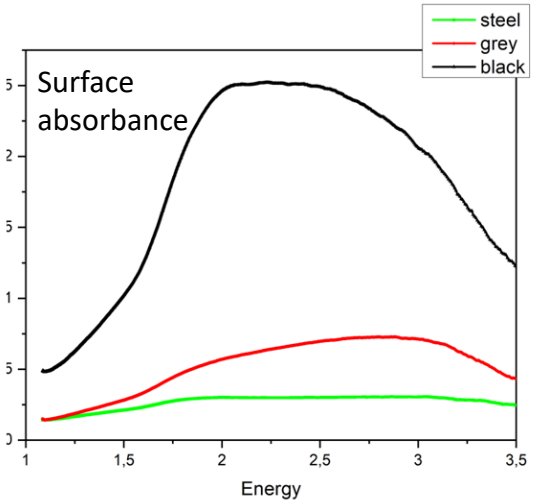

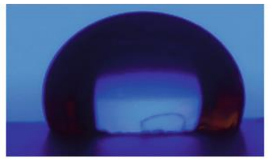

a

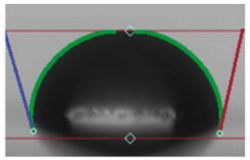

b

Preparation and analysis of thin films and surface nanostructures

Electron lithography

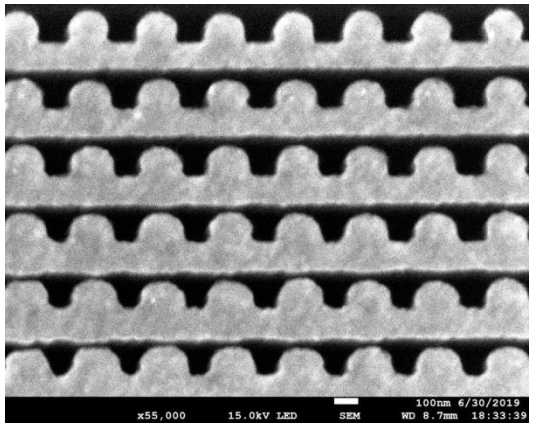

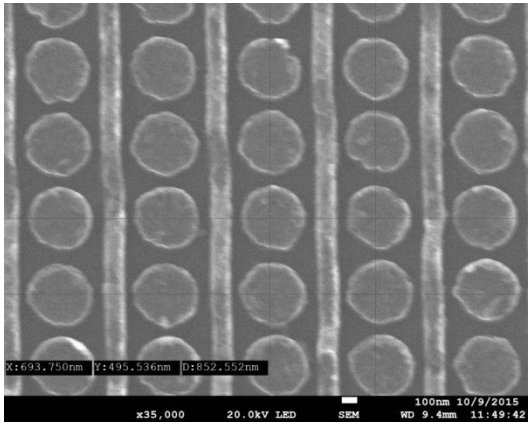

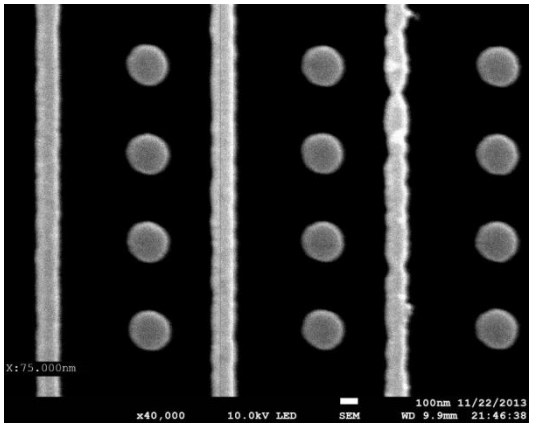

Preparation and analysis of thin films and surface nanostructures

Physical Vapor Deposition, Thermal Structurization, SPM imaging

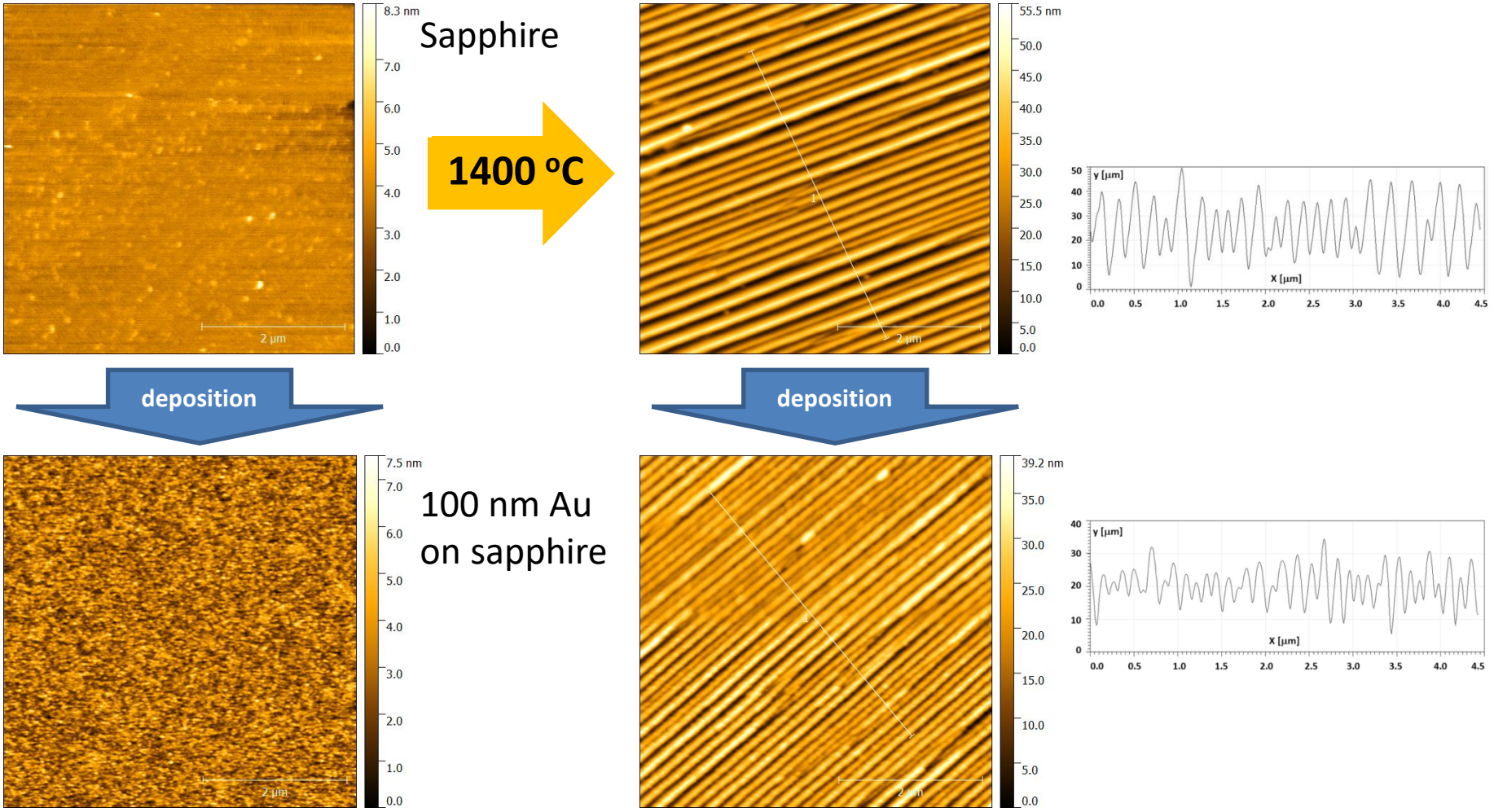

Scanning probe microscope (SPM)

Nazwa systemu pomiarowego	Skaningowy Mikroskop Próbnikowy (SPM)
Metoda badań	Mikroskopia sił atomowych (AFM) i metody pokrewne
Wyposażenie	•Mikroskop Park XE7 •Skaner 50x50 μm^2 •Przystawka SCM ze wzmacniaczem lock-in SR830 DSP •Stolik antywibracyjny •Kamera optyczna
Możliwości badawcze	•Obrazowanie nanostruktur powierzchniowych w modach kontaktowym i bezkontaktowym (cAFM, ncAFM) •Mikroskopia z detekcją fazową (PDM) •Mikroskopia sił bocznych (LFM) •Skaningowa mikroskopia pojemnościowa (SCM) •Określanie szorstkości powierzchni i rozmiarów nanostruktur

Wetting phenomena on solid surfaces

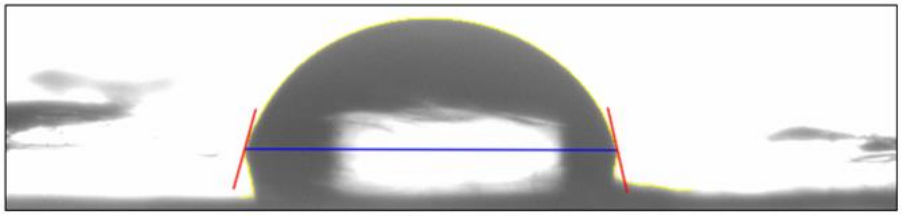

H_2O on HOPG

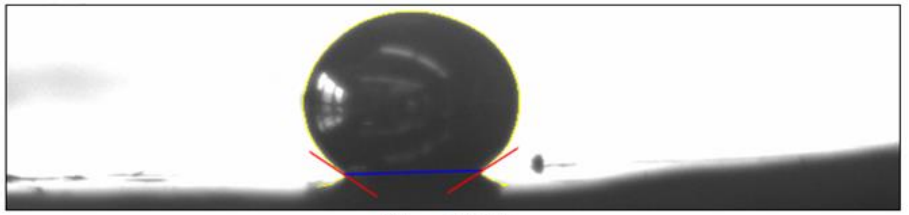

Hg on HOPG

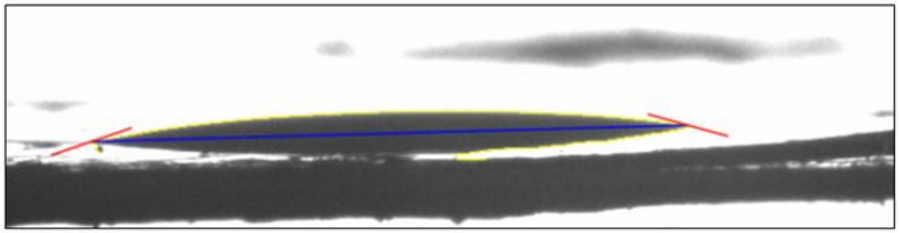

CCl_4 on HOPG

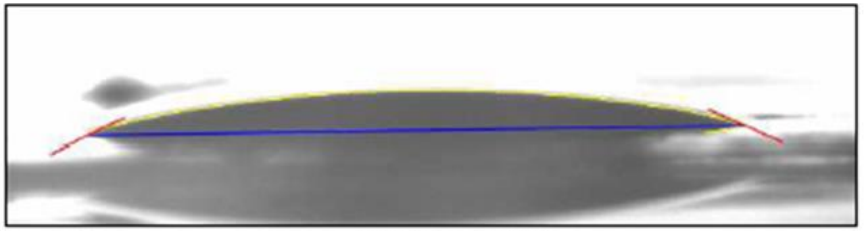

$C_6H_5NO_2$ on HOPG

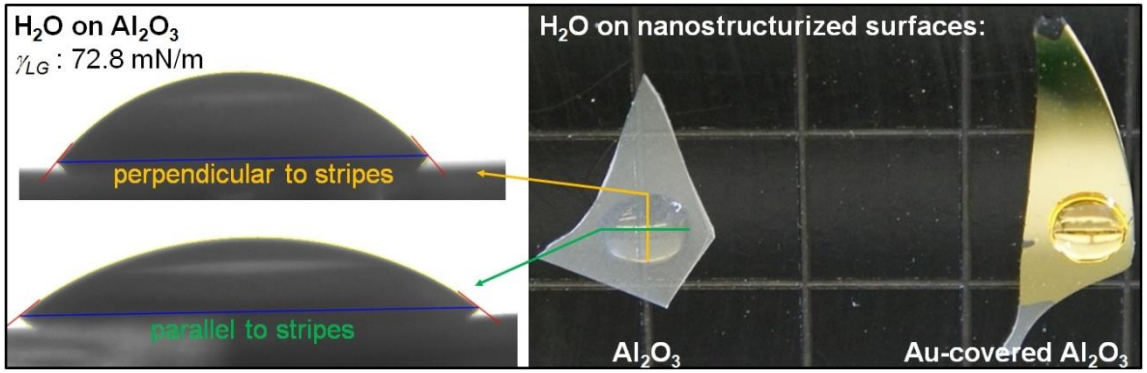

Wetting phenomena on solid surfaces and inside porous systems

Nazwa systemu pomiarowego	Goniometr Phoenix 300 SEO
Metoda badań	Obrazowanie kropli wiszącej oraz na powierzchni
Wyposażenie	•ręczny dozownik kropli •kamera optyczna •przystawka temperaturowa
Możliwości badawcze	•napięcie powierzchniowe •kąt zwilżania cieczy na powierzchniach ciał stałych •zakres temperatur od -40 do 30 °C

Nazwa systemu pomiarowego	Tensjometr Attension Sigma 700, Biolin Scientific
Metoda badań	Tensjometria mechaniczna
Wyposażenie	•zautomatyzowany pomiar siły •naczynie termostatyczne z kontrolerem temperatury od -20 do 200 °C
Możliwości badawcze	•napięcie powierzchniowe i międzywierzchniowe •kąt zwilżania •energia powierzchniowa •zwilżalność proszków •sedymentacja •siły adhezji

Nanomaterials for biomedical applications

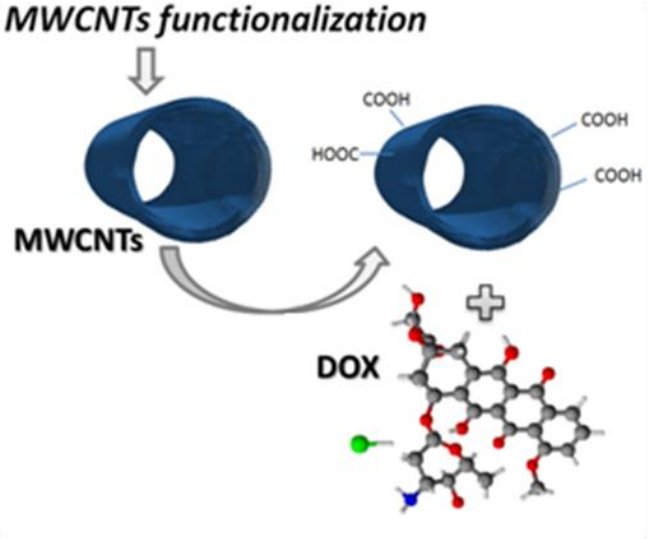

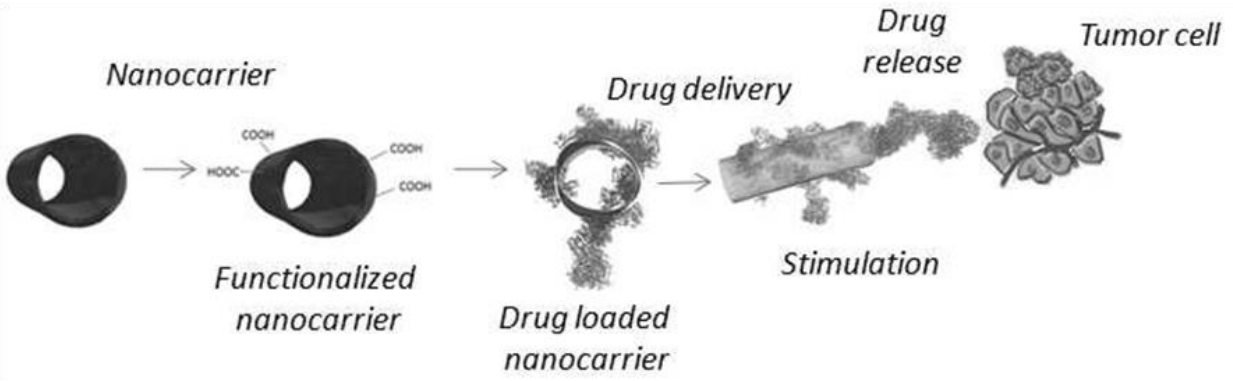

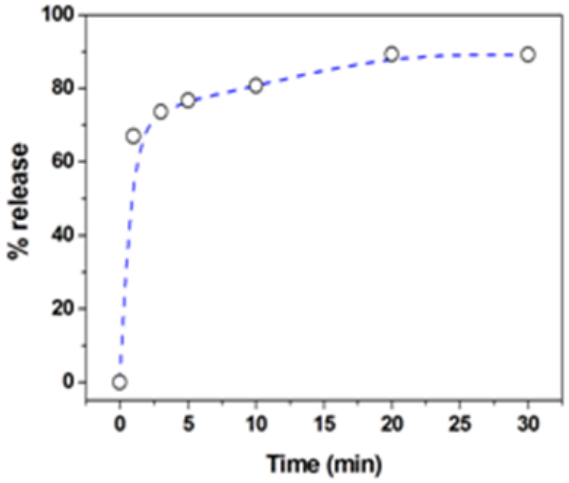

Release kinetics curve of DOX from mMWCNTs

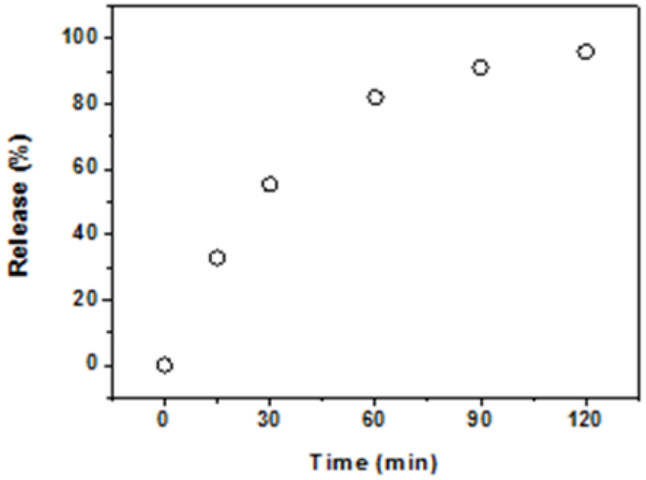

Release kinetics curve of doxorubicin from pCF

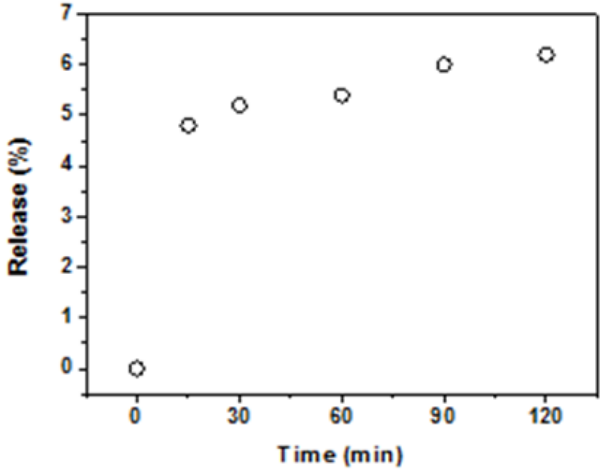

Release kinetics curve of doxorubicin from CF400

Carbon nanomaterials as dye carriers for enhanced photosyntesis and biomass production

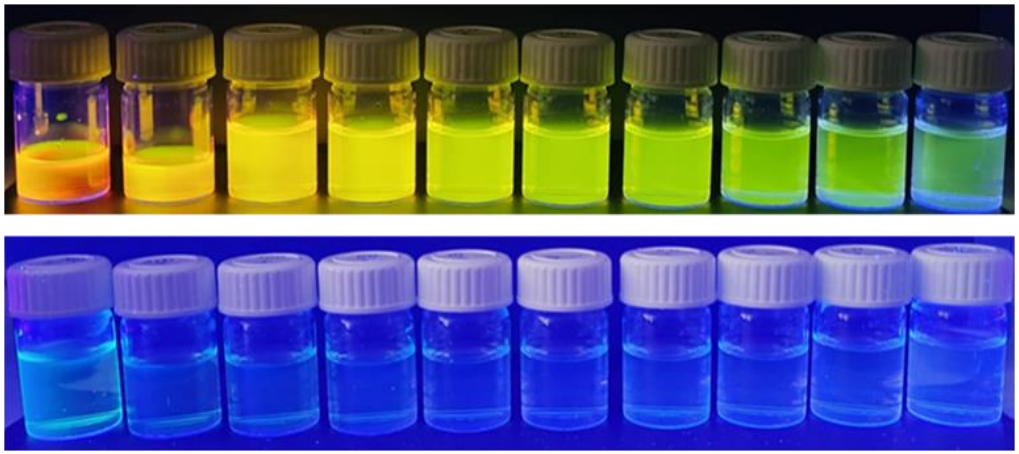

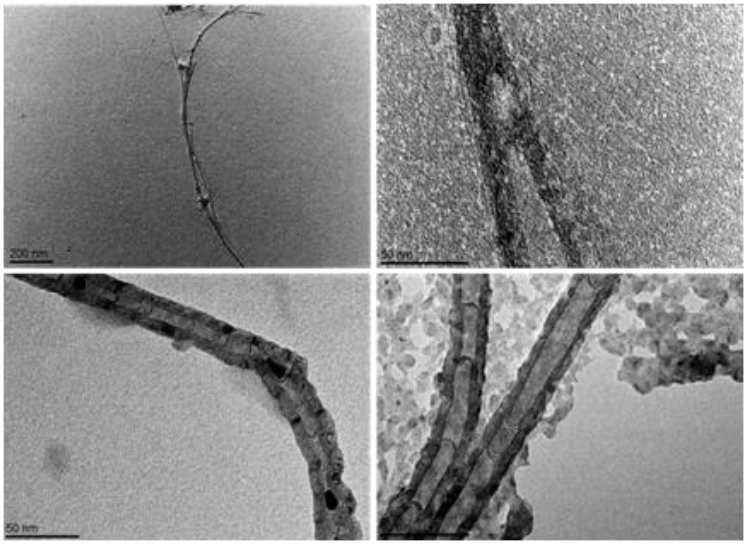

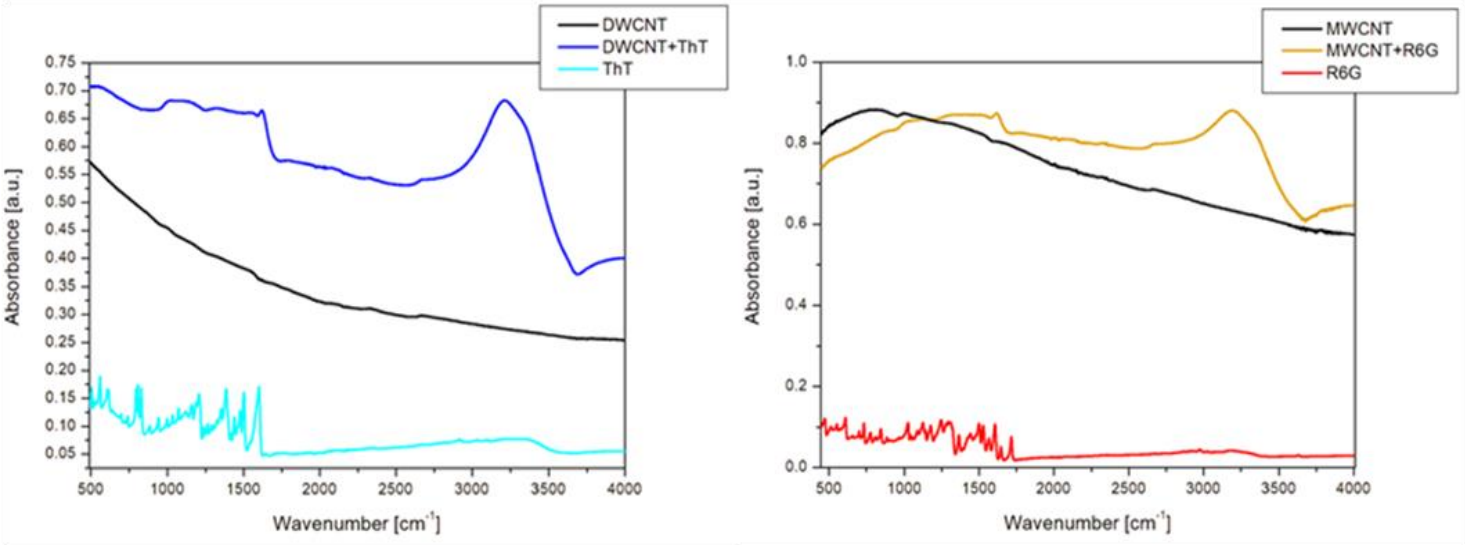

FTIR spectra showing Double-Walled Carbon Nanotubes (DWCNT) with Theaflavin (ThT) and Multi-Walled Carbon Nanotubes (MWCNT) with Rhodamine 6G (R6G). The shifts in the spectra confirm successful encapsulation of the dyes within the nanotubes.

Phase transitions in porous media (confined systems)

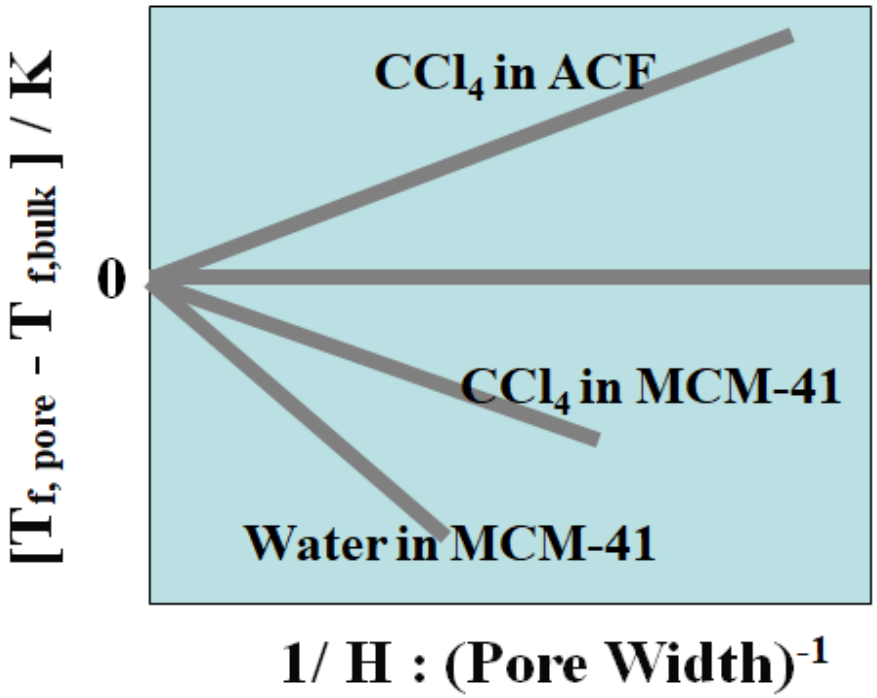

Experimental results from literature

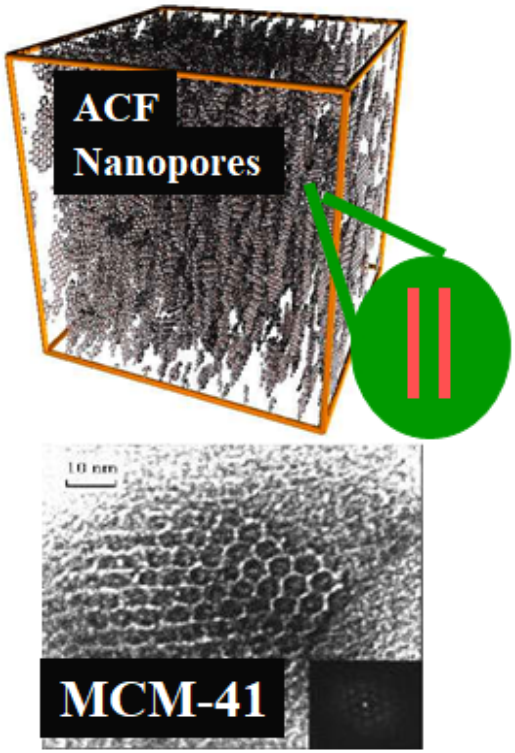

L.D. Gelb, K.E. Gubbins, R. Radhakrishnan and M. Sliwinska-Bartkowiak, "Phase Separation in Confined Systems", *Reports on Progress in Physics*, **62**, 1573-1659 (1999).

Theory of Corresponding States:

$$T_{f,pore}^{*} = f[H^{*}, \alpha, \sigma_{fw}/\sigma_{ff}] \approx f[H^{*}, \alpha]$$

$$T_{f,pore}^{*} = kT_{f,pore} / \varepsilon_{ff}; \quad H^{*} = H / \sigma_{ff}$$

$$\alpha = U_{fw} / U_{ff} = \rho_w \varepsilon_{fw} \sigma_{fw}^{2} \Delta / \varepsilon_{ff}$$

Melting temperature of substances in pores as a function of pore size and the parameter of host-guest interaction **α**

Quasi-high pressure effects observed in substances adsorbed inside porous systems

It is frequently observed that phase changes which only occur at high pressures or at low temperatures in the bulk phase take place in the confined phase at pressures that are orders of magnitude lower (bulk phase pressure in equilibrium with the confined phase) and at normal temperatures.

Examples of such phenomena include

- **high pressure chemical reactions,**
- **high pressure solid phases,**
- **high pressure effects in solid-liquid equilibria and effects on spectral properties.**

K. Kaneko et all, Langmuir, 1989,
W. Klein, E. Kumczeva, Science ,1995,
H. C. Turner, J. Chem. Phys. 2001.

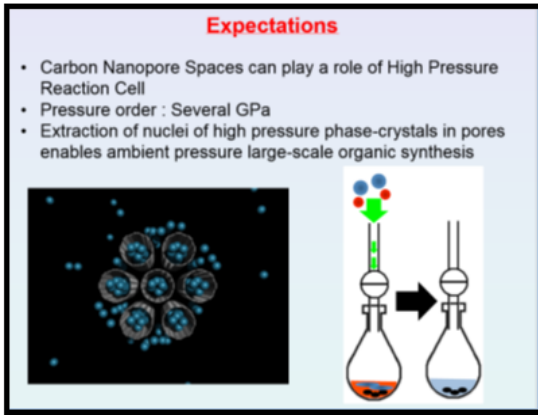

Deformation of porous matrix

Estimation of pressure in ACF pores (1.4 nm and 0.9nm)

For pitch-based mesoporous ACF the transverse compressive modulus E_T is about 2.9 GPa.*
Taking 0.13 as the value of $(\Delta d_{002} / d_{002})$ - the shrinkage in the interplanar distance in ACF from 3.78 Å to 3.30 Å, we estimate the approximate magnitude of P_N in ACF under water adsorption conditions:

$E_T = P_N / 0.13 \approx 2.9$ GPa
and $P_N \approx$ 377 MPa

for ACF 0.9 nm pore size we observed Δd_{002} -0.14 Å and $P_N \approx$ - 111 MPa
which is in qualitative agreement with our theoretical calculation for P_N of water in ACF of 1.4 and 0.9 nm pore size

For ACF + CCl_4 we observe the shift
Δd_{002} = 3.78 Å – 3.33 Å = 0.45 Å
$E_T = P_N / 0.12 \approx 2.9$ GPa
and $P_N \approx$ 345 MPa

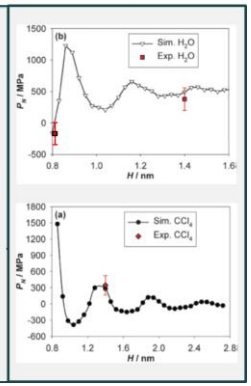

* S. Kawabata, *J. Text. Inst.*, 1990, 81, 432.
M. Śliwińska-Bartkowiak, H.Drozdowski et al. *Phys. Chem. Chem. Phys.*, 2012, 14, 7145–7153

High-pressure ice forms:

XRD patterns for ice confined inside the pores of KIT–6 (H = 9.3 [nm])

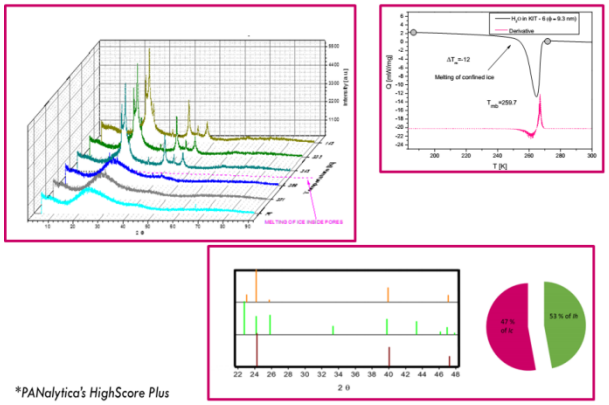

*PANalytica's HighScore Plus

STACKING DISORDERED ICE

❑ Traditionally, ice was considered to exist in two well-defined crystalline forms at ambient pressure: stable hexagonal ice (ice *Ih*) and metastable cubic ice (ice *Ic*)

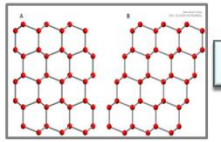

Stacking disordered ice, does not possess cubic nor hexagonal symmetry but it was recognised and identified to have the space group *P3m*.

❑ heterogeneous nucleation

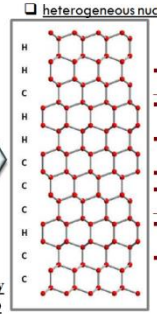

- re-crystallisation from high pressure phases
- heating of low-density amorphous ice
- heating of glassy aqueous solutions
- deposition of water vapour
- freezing of water and aqueous solutions
- freezing of nanometre scaled water clusters
- freezing of water in the confinement ?

*Malkin, T. L., Murray, B. J., Salzmann, C., Molinero, V., Pickering, S. J., & Whale, T. F. (2014). Stacking disorder in ice I. *Phys. Chem. Chem. Phys.*

Dielectric spectroscopy in a broad temperature range

Nazwa systemu pomiarowego	Układ do badań metodami spektroskopii dielektrycznej w szerokim zakresie temperatur
Metoda badań	Spektroskopia dielektryczna
Wyposażenie	•Analizator impedancji Solartron 1260 •Przystawka Dielectric Interface 1296 •Kriostat przepływowy LN_2/LHe z okienkiem do pomiarów optycznych •Kontroler temperatury ITC503S •Kondensatory do badań proszków i cieczy
Możliwości badawcze	•Pomiar stałej dielektrycznej i kąta strat •Wyznaczanie czasów relaksacji dielektrycznej •Badania przejść fazowych substancji czystych i uwięzionych w matrycach porowatych •Zakres temperatur od 10 do 300 K

Physical properties of liquid systems

Nazwa systemu pomiarowego	Lepkościomierz Kinematyczny SVM 3001 Anton Paar
Metoda badań	Metoda Stabingera: ASTM D7042, D445 z korekcją odchyleń, ISO 23581, EN 16896; ASTM D4052, ISO 12185
Wyposażenie	•cela do pomiaru gęstości •cela do pomiaru lepkości •układ szybkiego napełniania •automatyczna kontrola pomiaru
Możliwości badawcze	•Pomiary lepkości •Pomiary gęstości •Zakres temperatur od -60 do 135 °C •Szeroki zakres stosowalności: smary, paliwa, woski, oleje, ciecze proste

Ionic liquids adsorbed in mesoporous carbons

Systems studied:

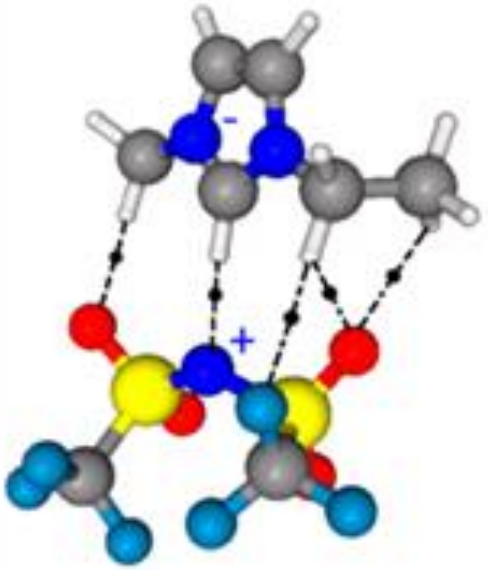

EMIN TFSI ionic liquid
(1-Ethyl-3-methylimidazolium bis(trifluoromethylsulfonyl) imide